

Review

Recent Advances in Photosensitizers as Multifunctional Theranostic Agents for Imaging-Guided Photodynamic Therapy of Cancer

Paromita Sarbadhikary, Blassan P. George[✉] and Heidi Abrahamse

Laser Research Centre, Faculty of Health Sciences, University of Johannesburg, Doornfontein, South Africa

✉ Corresponding author: blasang@uj.ac.za; Fax: 011 599 6448; Tel.: 011 599 6926© The author(s). This is an open access article distributed under the terms of the Creative Commons Attribution License (<https://creativecommons.org/licenses/by/4.0/>). See <http://ivyspring.com/terms> for full terms and conditions.

Received: 2021.05.08; Accepted: 2021.07.27; Published: 2021.08.26

Abstract

In recent years tremendous effort has been invested in the field of cancer diagnosis and treatment with an overall goal of improving cancer management, therapeutic outcome, patient survival, and quality of life. Photodynamic Therapy (PDT), which works on the principle of light-induced activation of photosensitizers (PS) leading to Reactive Oxygen Species (ROS) mediated cancer cell killing has received increased attention as a promising alternative to overcome several limitations of conventional cancer therapies. Compared to conventional therapies, PDT offers the advantages of selectivity, minimal invasiveness, localized treatment, and spatio-temporal control which minimizes the overall therapeutic side effects and can be repeated as needed without interfering with other treatments and inducing treatment resistance. Overall PDT efficacy requires proper planning of various parameters like localization and concentration of PS at the tumor site, light dose, oxygen concentration and heterogeneity of the tumor microenvironment, which can be achieved with advanced imaging techniques. Consequently, there has been tremendous interest in the rationale design of PS formulations to exploit their theranostic potential to unleash the imperative contribution of medical imaging in the context of successful PDT outcomes. Further, recent advances in PS formulations as activatable phototheranostic agents have shown promising potential for finely controlled imaging-guided PDT due to their propensity to specifically turning on diagnostic signals simultaneously with photodynamic effects in response to the tumor-specific stimuli. In this review, we have summarized the recent progress in the development of PS-based multifunctional theranostic agents for biomedical applications in multimodal imaging combined with PDT. We also present the role of different imaging modalities; magnetic resonance, optical, nuclear, acoustic, and photoacoustic in improving the pre-and post-PDT effects. We anticipate that the information presented in this review will encourage future development and design of PSs for improved image-guided PDT for cancer treatment.

Key words: Cancer diagnosis; Molecular imaging; Photodynamic therapy; Photosensitizers; Theranostics

Introduction

As per GLOBOCON report about 19.3 million new cases and 10 million cancer deaths have been estimated worldwide in 2020, being the first or second leading cause of death in most countries [1]. Moreover, many clinical studies have reported that the present COVID19 pandemic will further increase the burden of cancer-related mortality rate as a severe acute respiratory syndrome coronavirus 2 (SARS-CoV-2) infection increases the susceptibility

and severity of disease course of cancer patients [2]. It's almost 250 years of first detection of cancer and 60 years since the first approved cancer therapy, still, researchers worldwide are struggling to find a cure and/or improve the quality of life in cancer patients post-treatment while billions of dollars are spent annually on cancer research [3]. Even though much progress has been made in oncological research, there are still many issues that must be addressed to

improve cancer therapy and diagnosis. A lot of effort has been focused on two main aspects (a) novel and efficacious anticancer strategies which can overcome the severe side effects caused by conventional treatments, (b) innovative imaging approaches for early diagnosis and real-time functional monitoring to plan, evaluate, and monitor the treatment.

The context of this review is the utilization of photosensitizers (PSs) and their functionalized formulations for several conventional and advanced imaging modalities for the assessment of Photodynamic Therapy (PDT) outcomes. To the best of our knowledge, no systematic discussion has been published which summarizes several imaging modalities in combination with PDT or utilizing PSs as an imaging agent. This review highlights the specific applications and importance of imaging in PDT starting from the conventional fluorescence-guided PDT to more advanced X-ray Computed Tomography (CT), Magnetic Resonance Imaging (MRI), Single-Photon Emission Computed Tomography (SPECT), Positron Emission Tomography (PET), Ultrasound (US), and other optical imaging (OI) techniques combined with PDT for improved efficacies. With this background, the use of both optical and non-optical imaging techniques used for diagnostics as well as to assess PDT outcomes will be discussed in detail. Recently, the focus of advancement in PDT has been shifted towards novel strategies like designing and applications of activatable PS (aPS) which are activated under specific tumor microenvironment and/or stimuli. Several reviews have extensively discussed the important concepts, strategies, significant advances and rationale behind the designing of aPS [4–6]. This review will not focus on aPSs as a major topic and have included some relevant examples of aPSs which have been particularly utilized as PDT combined imaging agent. Further, this review will discuss only limited aspects of the PDT providing only an overall overview.

Photodynamic therapy: Overview

As an anticancer therapy, PDT is a clinically approved modality and has gained extensive attention owing to its minimal invasiveness, precise controllability, and high spatiotemporal accuracy with minimum side effects (Figure 1A). In principle, PDT is based on the photochemical process where photoactive drugs known as PSs are excited by light of appropriate wavelength (600–800 nm) to generate cytotoxic reactive oxygen species (ROS) leading to cancer cell death. The wavelength region between 600–800 nm is known as optical or therapeutic window for PDT, which exhibits significantly high

optical penetration depth in the tissue, as well as photons of this range have sufficiently high energy to excite the PS. Optical penetration depth of light in tissue is wavelength dependent, which represent distance at which the light intensity reduces to 0.37 of the initial intensity. Endogenous chromophores in tissues like oxyhemoglobin, deoxyhemoglobin, melanin, and water exhibit lowest absorbance in this region, thus having highest penetration depth in tissues. Therefore, due to wavelength-dependent scattering and absorption characteristics of endogenous chromophores, the optical penetration depth of light varies as < 0.5 mm at 400–430 nm, 1 mm at 500 nm, 2–3 mm at 630 nm, and 5–6 mm at 700–800 nm [7].

Mechanistically, PDT operates through type I and type II photochemical processes (Figure 1B). By the absorption of light of appropriate energy in the ground state PS (S_0) transforms to a short-lived excited singlet state (S_1 or $^1PS^*$). Following which either the $^1PS^*$ returns to its ground state with the emission of longer wavelength light (fluorescence) or can undergo intersystem crossing (ISC) to form a relatively long-lived triplet state (T_1 or $^3PS^*$) by spin inversion of the excited electron. $^3PS^*$ to S_0 is spin forbidden transition and thus is a very slow process. $^3PS^*$ can either relax back to ground state PS, emitting light (phosphorescence) or by transferring energy to other nearby molecules, which forms the basis of type I or type II reactions. The type I process is an oxygen (O_2)-independent reaction, in which the $^3PS^*$ directly reacts with the surrounding cellular biomolecules to form free radicals such as hydroxyl radicals ($\cdot OH$), superoxide anion radicals (O_2^-) and hydrogen peroxides (H_2O_2) via electron transfer. While type II is a highly O_2 -dependent process where the $^3PS^*$ directly transfers its energy to molecular 3O_2 to form highly reactive singlet oxygen (1O_2) [8–10]. Generation of ROS causes complex PDT induced tumor response involving direct tumor cell killing, microvascular damage to activation of innate and adaptive immune responses which altogether enhances the therapeutic outcome as represented in Figure 2. PDT induced irreversible oxidative damage in tumor cells leads to cell death predominantly via apoptosis and/or necrosis and to a lesser extent by autophagy. Tumor cell killing effect is further aggravated by vascular damage restricting O_2 and nutrient supply to tumor mass. Moreover, PDT mediated oxidative stress provokes a strong acute inflammatory reaction at the tumor site due to damaged and leaky tumor vasculature. This includes secretion of proinflammatory cytokines, activation of the complement pathways, and rapid recruitment of neutrophils, dendritic cells and macrophages at the

tumor site. Further, phagocytosis of tumor cell debris by phagocytic cells activates the adaptive immune response causing expansion of tumor-sensitized lymphocytes followed by their migration to a damaged tumor site resulting in the elimination of residual tumor cells [10]. Furthermore, emerging evidence has shown that PDT induced destruction of tumor stroma and/or microenvironment, increases tumoral drug penetration and can overcome cancer drug resistance and re-sensitize resistant cancer cells to standard therapies [9,11].

Despite its tremendous potential, application of conventional PDT has been restricted as adjuvant therapy and to only superficial tumors due to its inability to treat deep-seated tumors attributed to: poor penetration depth of visible light in tissues, inefficient accumulation of PS inside the tumor mass, tumor hypoxia and heterogeneity. In an effort to establish PDT as a frontline treatment modality and to enhance the therapeutic effect of PDT, innovative approaches are being exploited to circumvent the limitations in the currently used PDT model in clinics. The latest advancements of PDT for cancer therapy have been focused on improving light source to overcome penetration depth issues, stability and targeting ability of PSs, and tumor hypoxia (Figure 1A) [8,12–14].

Although not only PDT, all other conventional and advanced cancer therapeutics have evolved appreciably over the decades and resulted into significant improvements in treatment outcomes and

management of cancer patients. However, imaging plays an integral role in clinical cancer care by performing diagnosis, prognosis, screening, staging, treatment planning, monitoring to the assessment of treatment responses in relation to cure and treatment induced toxicity along with improving the basic understanding of the complex cancer biology at molecular to the cellular level. Innovations in single-model and multimodal conventional and novel imaging modalities offer promising and exceptional opportunities towards targeted, precision, and personalized cancer therapy. The following section provides a comprehensive overview of clinically approved imaging techniques in cancer therapy and their unique imaging potency and intrinsic limitations. Further, the utility of these imaging techniques in planning, designing, monitoring, and assessment, for enhancing the effectiveness of PDT outcomes have been briefly discussed in the following section.

Cancer Imaging Modalities

Other than advancement in targeted anticancer therapies, another field in which tremendous efforts are being investigated is advanced cancer imaging modalities and development of multi-functional theranostic systems for combined cancer diagnosis and therapy. Medical imaging is an indispensable component of clinical cancer treatment paradigm and plays an important role in all phases of cancer management starting from screening, detection,

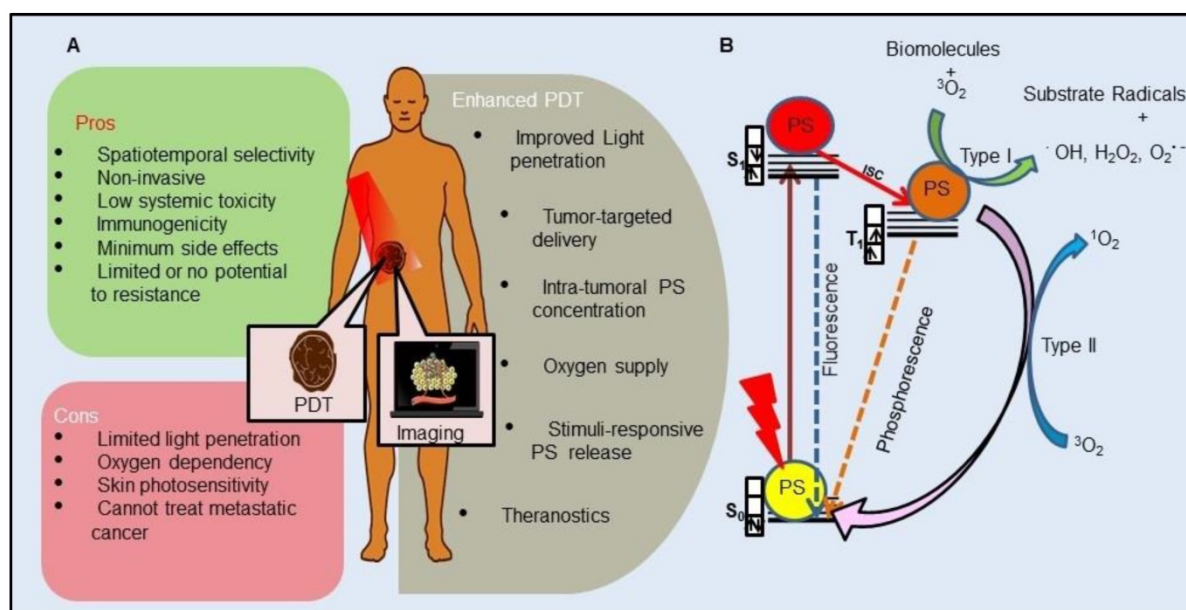


Figure 1. General schematic representation of Photodynamic Therapy (PDT): **A.** Illustration of PDT where photosensitizer (PS) serves as both an imaging agent and a therapeutic agent. Advantages, disadvantages, and different strategies to enhance PDT of cancer. **B.** Modified Jablonski diagram showing the principle of PDT: Absorption of light energy by ground state PS (S_0) results into its excitation to singlet $^1PS^*$ (S_1). Intersystem crossing (ISC) transforms the S_1 to excited triplet $^3PS^*$ (T_1). T_1 either through electron transfer to cellular biomolecules (Type I) and/or via direct energy transfer to 3O_2 (Type II) results in the production of Reactive Oxygen Species (ROS) to induce cell death.

staging, prognosis, therapy planning, guidance and finally to monitoring therapy response, recurrence and palliation. Main requirements of cancer diagnostics include minimal to non-invasiveness, imaging convenience without tissue destruction, real-time monitoring, functioning over wide ranges of time and size, and should furnish morphological, structural, metabolic and functional information from molecular to cellular to organ to organism levels [15,16]. Over the years, cancer imaging techniques have made significant progress from conventional methods yielding structural information to more advanced and relatively recent functional and molecular imaging technologies. Traditional imaging methods, such as MRI, CT and US basically provide structural information primarily size, shape, morphology and location of internal body parts. These imaging techniques furnish information about physical or anatomical abnormalities in the structure like bones, organs, and blood vessels without providing any detailed information thus often needed to confirm a diagnosis by invasive methods like biopsy. Moreover, tumors need to attain a certain size to be imaged anatomically which limits the early detection of cancer and cannot be used for real-time monitoring during the therapeutic regime. While functional imaging which is frequently associated with molecular imaging examines the physiology of diverse and dynamic bioprocess at the cellular or organ level like detection of changes in blood circulation, diffusion, perfusion and bio-distribution of drugs. Functional imaging techniques include

diffusion MR techniques, perfusion weighted imaging, functional MRI and pharmacological MRI. Molecular imaging is a more advanced and emerging biomedical research field that enables visualization, characterization and quantification of biological processes taking place at the molecular, subcellular and cellular levels within the living system [16–18]. Molecular imaging allows repeated *in vivo* detection of various critical molecular features of cancer hallmarks, such as proliferation, metabolism, hypoxia, angiogenesis and apoptosis. More importantly, molecular imaging has a significant role, in personalized cancer treatment, owing to its involvement in early detection and/or real-time monitoring of molecular changes occurring in cancer cells or tissue and consequently, identifying changes in individual patients both at pre- and post-treatment. This further allows for planning and choice of most appropriate therapy, doses etc., depending on the stage and biological features of the tumor [18,19].

Molecular imaging includes US, MRI, CT, OI, nuclear imaging involving PET and SPECT. Other than these techniques, some more advanced imaging modalities like photoacoustic imaging (PAI), Surface-enhanced Raman Scattering (SERS) imaging, upconversion luminescence (UCL) and cerenkov luminescence imaging are gaining interest in cancer management. However, each imaging modality has pros and cons, based on their unique sensitivity, spatial resolution, temporal resolution, penetration depth etc., (Table 1). Thus, no single modal imaging technique is sufficient enough to acquire all the

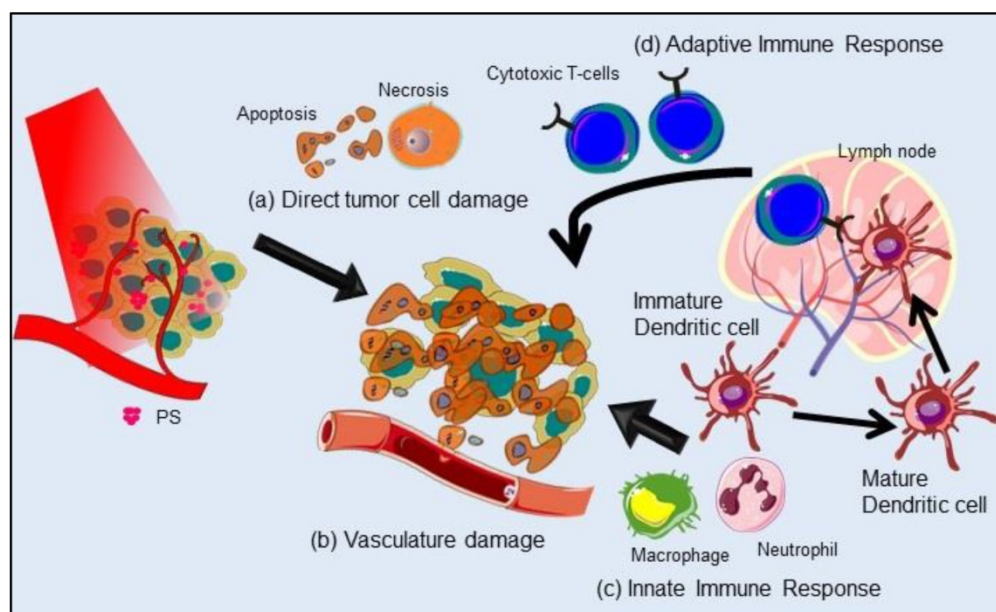


Figure 2. Photodynamic Therapy (PDT) induced cellular effects and immune responses: Generation of reactive oxygen species induces (a) direct tumor cell killing predominantly via apoptosis and necrosis, and (b) damages tumor vasculature. In addition, PDT effect is further potentiated by activating both (c) innate and (d) adaptive immune responses against tumor, further eliminating the residual tumor cells. PS: Photosensitizer.

required information and the choice of imaging technique primarily depends on the biological system being studied and the physiological question being asked [16]. A multimodality imaging technique combined with two or more imaging methods can overcome the intrinsic limitations of each modality. Furthermore, this approach results in obtaining complementary, effective, high quality, and accurate information about the anatomical, physical, structural and physiological function for cancer diagnosis and treatment. Moreover, clinical implementation of combined PET/MR and PET/CT scanners, have made the implementation of multimodal imaging more feasible [17,20].

Role of Imaging in Photodynamic Therapy

Like any other therapy, the success of PDT efficacy is also based on the accuracy of pre- and post-PDT dosimetric and monitoring parameters for predicting therapeutic response and planning of subsequent therapeutic schedules. PDT based dosimetry parameters include: (1) pretreatment tumor parameters, such as tumor size, vascular density, oxygen distribution at the tumor site and inter- and intratumoral heterogeneity, (2) real-time therapeutic monitoring parameters including uptake and concentration of PS at the tumor site, its intra and extracellular spatial localization, light dose, and distribution, and (3) post-therapy monitoring of response, recurrence and palliation. Assessment of therapeutic outcome by employing imaging techniques post PDT treatment in tumor tissue provides evidence of necrosis, apoptosis, tumor damage and blood vessel occlusion. Due to the intrinsic fluorescence property of PS, OI based on PS fluorescence imaging had become the standard imaging technique in every stage of PDT, from detection to treatment planning and the outcome in clinical settings. As compared to conventional imaging modalities fluorescence-guided imaging technique offers several advantages of better spatial and temporal imaging resolution along with being a much safer imaging modality. However, fluorescence

imaging limits the imaging depth up to few micrometers, thus can provide information of superficial structures only and fails to provide information in the 3D tumor volume. This inherent limitation of fluorescence imaging recommends the importance of other imaging modalities and/or multimodality imaging which can complement the uniqueness of fluorescence imaging by depth and volume resolved imaging approaches [21,22]. Pre and post PDT treatment and diagnostics with most commonly used clinical imaging techniques PET, MRI and CT provides significant information related to tumor localization and volume. However, without the use of exogenous contrast agents, these imaging methods suffer from the limitation of lack of resolving power of microcirculatory activity, thus makes it difficult to predict the actual dose required for the treatment outcome. Therefore, as mentioned in the previous section and Table 1, each and every imaging modality has certain strengths and limitations, and the choice for single or combination of imaging techniques in PDT entirely depends on the specific and relevant information required at clinical level. Table 2 represents conventional CT, PET, MRI, and advanced US, PAI, Optical Coherence Tomography (OCT), Fluorescence imaging (FLI) and other imaging techniques that have been successfully used in preclinical and clinical settings for the assessment of various structural and functional information to guide, monitor and evaluate PDT responses [11,21,22]. The relationship between structural, functional and molecular imaging approaches and their roles in pretreatment planning, monitoring therapy, and assessment of outcomes are schematically presented in Figure 3. As already mentioned, every imaging modality suffers from their intrinsic drawbacks of resolution, sensitivity and specificity. Thus, multimodal imaging and/or PDT combined imaging has the potential to provide optimism for the future of imaging in PDT and development of personalized patient treatments.

Table 1. Characteristics of clinical molecular imaging modalities in oncology.

	PET	SPECT	CT	MRI	US	OPTICAL
Signal Used	High-energy γ -ray	Low-energy γ -ray	X-rays	Radio waves	High-frequency sound waves	Visible light or near-infrared waves
Contrast agents/Tracers	β^+ emitting Radioisotope	γ - emitting Radioisotope	Krypton, Xenon, Barium and iodinated molecules	Gadolinium chelates/ superparamagnetic agents (SPIONs)	Microbubbles	Fluorescent probes/ dyes
Sensitivity^a (mol/L)	10^{-11} – 10^{-12}	10^{-10} – 10^{-11}	Not well characterized	10^{-3} – 10^{-5}	Not well characterized	10^{-9} – 10^{-12}
Spatial Resolution^b	1–2 mm	1–2 mm	50–200 μ m	25–100 μ m	50–500 μ m	2–3 mm
Temporal Resolution^c	10 seconds to minutes	Mins	Mins	Mins–Hrs	Sec–Min	Sec–Min
Depth of Penetration	No limit	No limit	No limit	No limit	mm–cm	< 1 cm

	PET	SPECT	CT	MRI	US	OPTICAL
Advantages	High sensitivity, can be used for whole body imaging		High resolution, can be used for whole body imaging, fast acquisition time	High spatial resolution, no ionizing radiation, high soft tissue contrast	Fast acquisition time, real-time imaging, no ionizing radiation, cost-effective	Fast acquisition time, no ionizing radiation, real-time imaging, high sensitivity, cost-effective
Disadvantages	Ionizing radiations, low resolution, expensive, long acquisition time		Ionizing radiations, low sensitivity, poor soft tissue demarcation	Poor sensitivity, long acquisition time, expensive	Poor contrast, low resolution	Low Resolution

*Sensitivity is the ability of imaging technique to detect or identify the presence of a molecular probe when it is truly present, relative to its background.

^bSpatial resolution is a measure of the accuracy or detail of image. It is mainly based on its detection ability to distinguish two adjacent structures as separate entities.

^cTemporal resolution is the frequency at which the images are recorded or captured. It is also represented as single acquisition time.

PET: Positron Emission Tomography; SPECT: Single-Photon Emission Computerized Tomography; CT: Computed tomography; MRI: Magnetic Resonance Imaging; US: Ultrasound

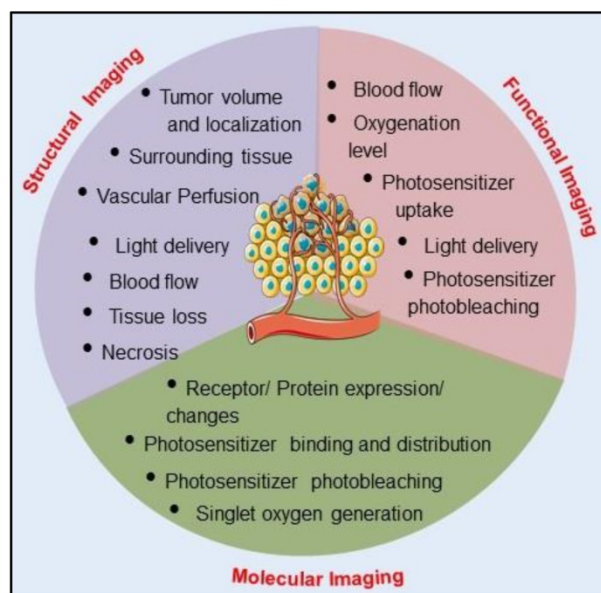


Figure 3. A schematic illustration depicting the roles of structural, functional and molecular imaging in guiding pre-treatment planning, therapy monitoring, and outcome assessment in Photodynamic Therapy.

Table 2. Summary of clinically relevant oncology informations provided by different imaging modalities to guide, monitor and evaluate Photodynamic Therapy responses in preclinical and clinical settings.

Imaging Modality	Pre and Post treatment Information
Endoscope-coupled FL, US, OCT	Tumor localization in hollow tube organs
CT	Tumor localization Necrosis and surviving tumor volume
MRI	Tumor volume Necrosis and histopathological analysis Vascular perfusion and permeability
PET	Tumor volume and localization Tumor hypoxia Necrosis and surviving tumor volume
OCT	Microscopic resolution of Tumor volume and margin delineation of superficial tumors
Laser Doppler imaging and Angiography	Vascular perfusion and blood flow velocity
OI	FL based PS uptake and photobleaching mediated treatment response Singlet oxygen luminescence (SOL)
US	Tumor volume and localization Necrotic and apoptotic tumor fraction Vascular density, perfusion and blood flow velocity Image-guided fiber placement
PAI	Vascular structure and density PS uptake and distribution PS photobleaching rate Dynamics of blood oxygen saturation and partial pressure of oxygen

PET: Positron Emission Tomography; SPECT: Single-Photon Emission Computerized Tomography; CT: Computed tomography; MRI: Magnetic Resonance Imaging; US: Ultrasound Imaging; FL: Fluorescence Imaging, OI: Optical Imaging; OCT: Optical Coherence Tomography; PAI: Photoacoustic Imaging; PS: Photosensitizer.

Theranostics: “Multifunctional Agents” for Image-guided Photodynamic Therapy

Application of Photosensitizers in Photodynamic Therapy and Imaging

In PDT, other than light dose and oxygen concentration, PSs play a critical role in the photochemical reactions to dictate the overall therapeutic outcome of PDT. Ideal PS must possess several ideal photophysical, chemical and pharmacokinetic properties to determine their application and efficiency as PDT agents. Ideally a PS should be in its chemically pure form with high storage stability. Photophysical characteristics of ideal PS should include strong absorption in the optical window region, substantially high triplet state and ROS quantum yield upon irradiation. It should also have preferential uptake by tumor tissue, minimal dark toxicity and rapid clearance from normal tissues to minimize the phototoxic side effects [23]. Most of the PSs used in PDT of cancer are based on the tetrapyrrole macrocyclic structure having extended π -electron systems responsible for their unique photophysical and photochemical properties. As illustrated in Figure 4 these photophysical and photochemical properties can be strategically tuned by: (i) chemical modification of the main macrocyclic porphyrin ring, (ii) introducing various functional groups/substituents as peripheral modification and (iii) coordination of metal ions in the centre of tetrapyrrolic ring [24]. Although photophysical and photochemical properties of PSs can be easily modified by chemical manipulation, while on the other hand, their pharmacokinetic profiles cannot be easily controlled. As shown in Table 3, numerous PSs are commercially available and have received clinical approval or have entered clinical trials for the treatment of various types of cancer. Despite several natural and synthetic PSs have been reported, not many PS meets all the required ideal properties thus

significantly limits their clinical use. The rationale designing of novel PS with desirable properties remains a big challenge. In recent years, several innovative PS designs and strategies are being explored to improve the treatment of deep-seated or thick tumors, stability and targeting ability of PSs, ROS production efficiency, tumor hypoxia, aPSs and nanosystem-based PS formulations for improving PDT efficacy [8,23,25–30].

Furthermore, utilization of PSs are not restricted solely to therapeutic PDT purpose. Being photoactive molecules, many PSs are inherently brightly fluorescent with their fluorescence emission in far red

or Near Infrared Radiation (NIR) region of electromagnetic spectra. Hence, PSs holds promise for *in vivo* FLI and is generally employed to monitor tumoral PS uptake and fluorescence-guided surgery (FGS) as is already approved for both bladder and brain cancers in Europe. In addition, FLI also allows follow-up PDT to remove any residual tumor cells that could cause recurrence and evaluating the outcome of treatment. Thus, the fluorescence property of PSs aids in useful dosimetric parameters like determining PS localization and uptake by tumor tissue in real-time and post PDT monitoring [22,27].

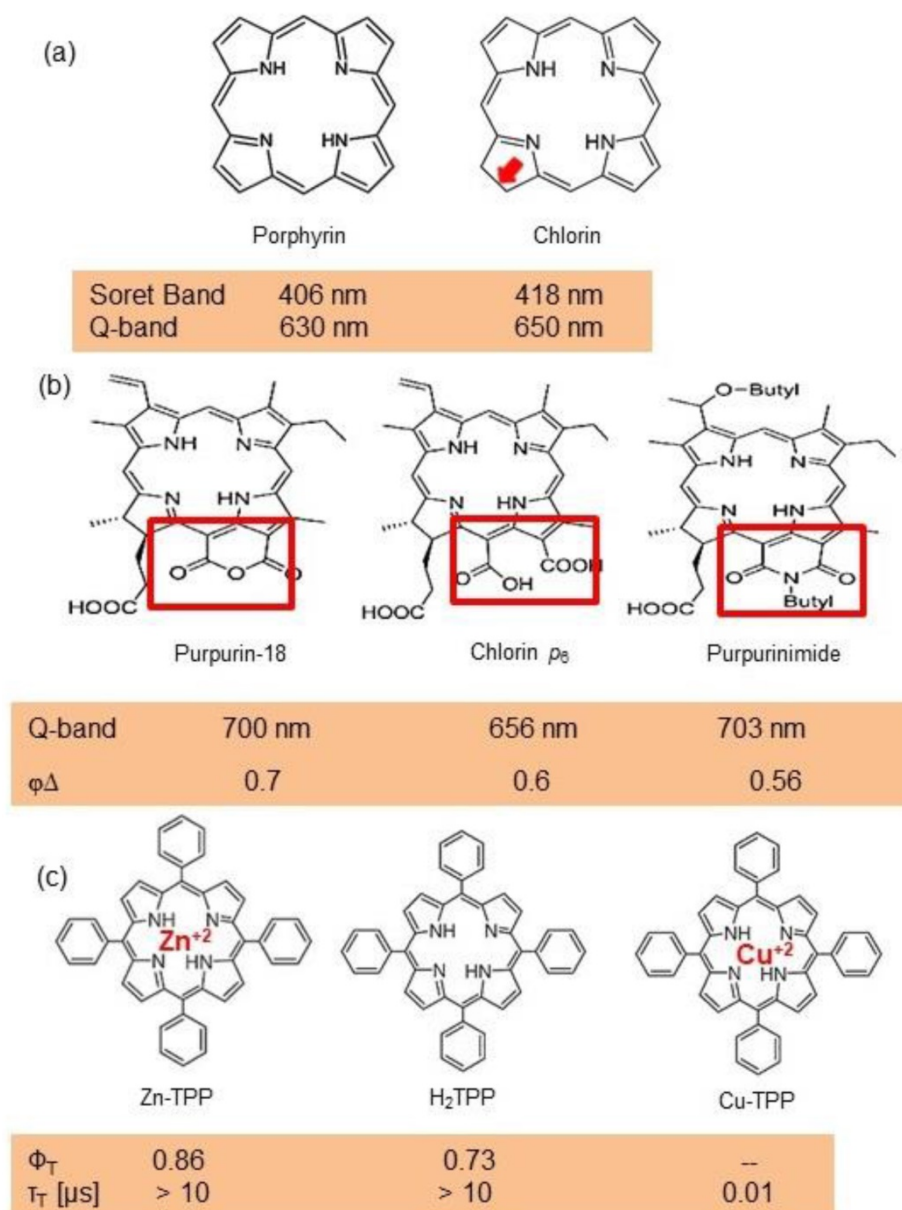
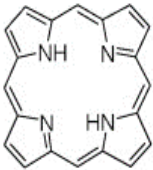
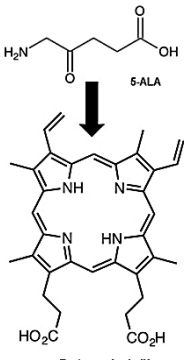
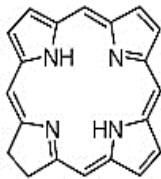


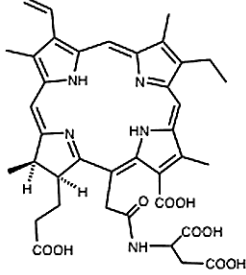
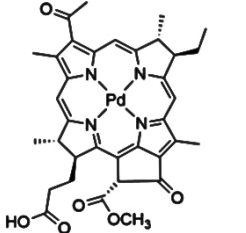
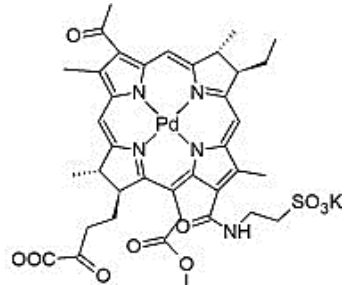
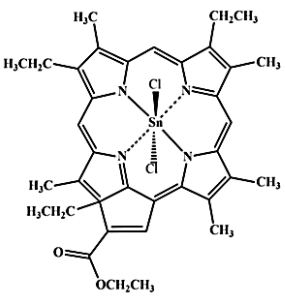
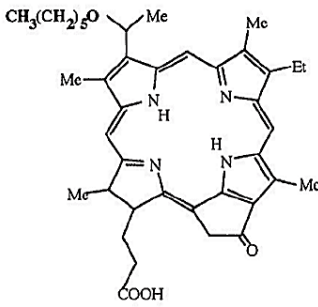
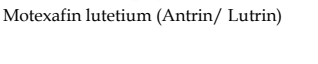
Figure 4. Chemical modifications of photosensitizer molecules with resulting photophysical and photochemical changes: (a) reduction of main macrocyclic porphyrin ring results in red shift of Q band of tetrapyrrole photosensitizer, (b) peripheral modification and (c) central metal coordination of tetrapyrrole ring induce changes in singlet oxygen quantum yield ($\phi\Delta$), triplet quantum yield (Φ_T) and triplet state lifetime (τ_T) depending on the type of side groups and central metal (diamagnetic or paramagnetic). Soret band: The strong absorption band of PS in the blue wavelength region of the visible spectrum due to the S_0 to S_2 transition. Q band: The weak absorption band of PS in longer wavelength region i.e. red or far red, due to S_0 to S_1 transition. $\phi\Delta$: Quantitative measure of PS efficiency to convert O_2 into 1O_2 upon photoexcitation. Φ_T : Number of PS molecules that undergoes singlet to triplet state transition with per photon absorption. PS: Photosensitizer

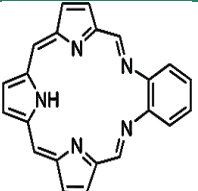
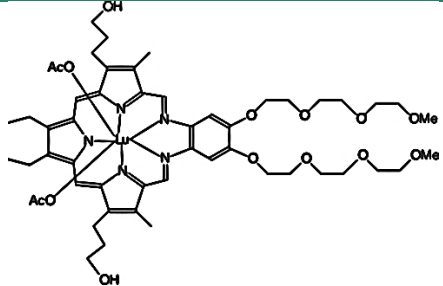
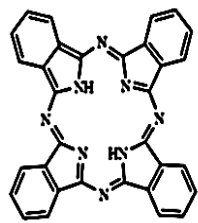
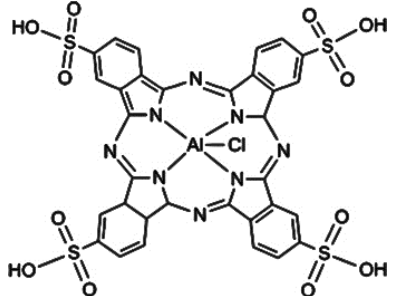
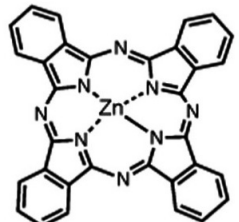
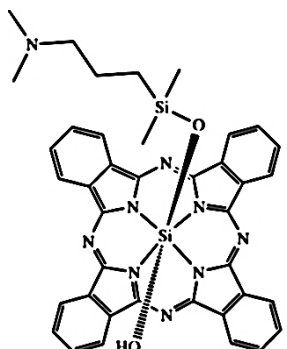
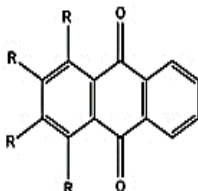
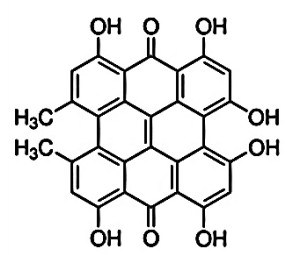
With the advancement in medicine, drug designing has revolutionized from the utilization of different drugs for therapy and diagnostics separately to theranostics by integration of therapeutic and diagnostics potential into a single drug molecule [31]. In 1998, Funkhouser coined the term “Theranostic” defining those materials that combine both therapeutic approach and diagnostic imaging in a single entity, so that both the agents are delivered at

the same time will show the same biodistribution pattern [31,32]. The theranostic field has the advantage of tuning the therapy and dose by gaining the ability to image and monitor the diseased tissue, delivery kinetics, and drug efficacy. Thus, due to its real-time monitoring of therapeutic outcome, theranostics have advanced in the biomedical field for the effective and personalized treatment approach [31].

Table 3. List of photosensitizers approved or in clinical trials for Photodynamic Therapy and diagnosis in oncology.

Class	Examples	λ_{max}	Clinical Approval
A. Tetrapyrrole based			
<i>(i) First generation</i>			
Porphyrin 	(a) Porphimer sodium (photofrin)	630 nm	Approved-Bladder cancer, Endobronchial cancer, Esophageal cancer, Lung cancer, Barrett's esophagus, cervical cancer In clinical trial- Brain cancer diagnosis
<i>(ii) Second generation</i>	(a) 5-Aminolevulinic acid (Levulan)	635 nm	Approved- Non-melanoma skin cancers, Basal cell carcinoma, Squamous cell carcinoma In clinical trial- Brain cancer diagnosis and guided resection
Porphyrin precursor 	(b) Hexaminolevulinic acid hydrochloride (Hexvix®)	635 nm	Bladder cancer diagnosis
	(a) 5,10,15,20-Tetrakis(3-hydroxyphenyl) chlorin/ Temoporfin (Foscan)	652 nm	Approved- Head and neck, Prostate and Pancreatic cancers
	(b) Mono-L-aspartyl chlorin e6 / Talaporfin (Laserphyrin)	664 nm	Approved- Lung cancer, Malignant gliomas

Class	Examples	λ_{max}	Clinical Approval
Bacteriopheophorbide	 <p>(a) Palladium-Bacteriopheophorbide (WST09)/ Padoporfin (Tookad)</p>  <p>(b) Bacteriopheophorbide (WST11)/ padeliporfin (Stakel)</p> 	763 nm	Approved- Prostate cancer
Purpurin	<p>Tin ethyl etiopurpurin/ Rostaporfin (Purlytin)</p> 	664 nm	In clinical trials- Basal cell cancer, Kaposi's sarcoma, Prostate cancer, Breast adenocarcinoma
Pheophorbide	<p>2-(1-Hexyloxyethyl)-2-devinyl pyropheophorbide-a / PhotoChlor</p> 	665 nm	In clinical trials- Basal cell carcinoma, Esophagus, Skin, Mouth and Throat cancers, Cervical intraepithelial neoplasia
Texaphyrin	<p>Motexafin lutetium (Antrin/ Lutrin)</p> 	732 nm	In clinical trials- Prostate, Breast, Cervical, Brain, Skin and Superficial cancers

Class	Examples	λ_{max}	Clinical Approval
 <p>Porphyrin related-Phthalocyanine (Pc)</p>	 <p>(a) Aluminum phthalocyanine tetrasulfonate chloride (Photosens)</p>	676 nm	In clinical trials- Stomach, Skin, Lip, Oral, and Breast cancers
 <p>(b) Zinc phthalocyanine</p>	 <p>(b) Zinc phthalocyanine</p>	676 nm	In clinical trials- Skin cancer, Squamous cell carcinoma
 <p>(c) Silicon Phthalocyanine</p>	 <p>B. Non-Porphyrin based Hypericin</p>	675 nm	In clinical trials- Skin cancer
 <p>Anthraquinone</p>		600 nm	In clinical trials- Cutaneous T-cell Lymphoma
<p>Cyanine</p>	<p>Indocyanine green (IR125)</p>	695-780 nm (Concentration dependent)	In clinical trials- Imaging-guided detection and PDT

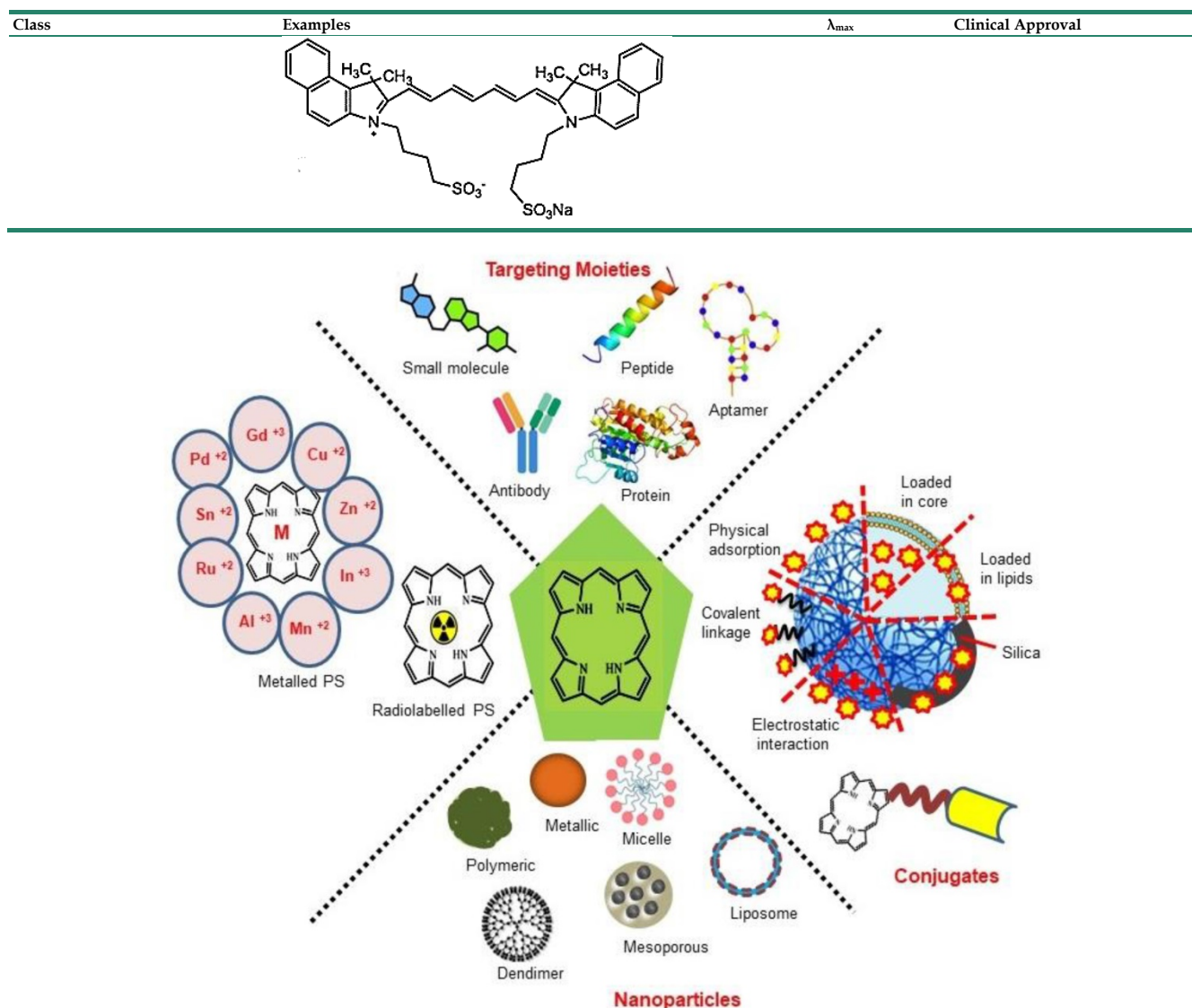


Figure 5. The structural designing of photosensitizer for therapy and imaging: Non metallated and metallated (radioactive or nonradioactive isotope) in the form of conjugates, linked with targeting moiety and nanoparticles for application in image-guided Photodynamic Therapy.

Traditional theranostic agents are basically simple combinations of imaging and therapeutic agents which are always used for both therapeutic effects and imaging signals. The drawbacks of these theranostic agents are its limited signal-to-noise ratio (SNR) and lack of selectivity or specificity in the disease sites. To overcome this issue, an activatable theranostic approach is being researched where an inactive agent could be specifically turned on at the target site by certain stimuli or reactions for simultaneous diagnostics and therapeutic application [33,34]. These activatable theranostic agents are endowed with a lower limit of detection, real-time detection of biomarkers, lower toxicity to the normal tissues, higher drug bioavailability and higher SNR [34]. In recent years, optical-based phototheranostics have gained increasing attention, due to the advantages of minimal invasiveness, local treatment

and spatio-temporal delivery of light reducing the collateral damage to normal surrounding tissues [35].

Although the concept of phototheranostics is recent, PDT already has proven theranostic applications due to the uniqueness of PSs fluorescence property, thus combining both therapeutic and imaging agent in a single molecule. As already discussed, fluorescence-based imaging in PDT has also shown to have multiple significance including diagnostics, dosimetry, monitoring, treatment assessment, therapy guidance and mechanistic studies [21]. FLI can provide cellular-level information with high sensitivity, however its widespread application in imaging field is limited due to poor penetration depth of light in tissues and low resolution. But this has not discouraged the use of PSs as theranostic agents due to their several favorable features like preferential uptake in tumors, relatively

low *in vivo* toxicity and more importantly its ease and straightforward functionalization chemistry. Thus, rationale designing with PSs, their derivatives, metallated counterparts and nanoformulations are actively being explored for several other imaging modalities like PET, SPECT, MRI, US, PAI, CT etc. for image-guided PDT (Figure 5) [3,11,36–39]. Figure 5 shows some representative designing strategies of PS for theranostics, this includes (1) metallated, non metallated and radiolabelled PS molecules, (2) nanoformulations fabricated using organic, inorganic, lipid and protein compounds, and (3) free or nanoparticle-based PS conjugated with targeting moieties to specifically target the tumor tissues. Targeting moieties including proteins (mainly antibodies and their fragments), peptides, nucleic acids (aptamers) and other small molecules are specifically used to guide PSs to specific tumor tissues. PS conjugates includes conjugating the free PS and/or decorating their nanoformulations with functional and targeting moieties.

Optical Imaging Combined Photodynamic Therapy

Over the past decades, diagnostic imaging has gained interest and has advanced steadily for the improvement and management of cancer patient care. As an alternative to conventional imaging modalities, OI techniques employing light (usually visible) to extract diagnostic information from light–tissue interactions have emerged as a safe and non-invasive technique for *in vivo* imaging [40]. Further, in comparison to the conventional imaging modalities certain interesting features such as ease of detection, high spatial and temporal resolutions, real-time evaluation and availability of a wide variety of light activated contrast agents uniquely make the OI platform an advantageous tool for clinical diagnosis and surgical applications [41]. Advancements in technologies have upgraded imaging of tumor lesions due to improved tissue penetration, sensitivity, and specificity by optical methods [41,42]. Due to the inherent fluorescence property of PS, their free form or the nanoformulations are widely used for *in vivo* conventional FLI in combination with real-time monitoring of surgery and targeted PDT by observing the PS accumulation. Better insight into the photophysical properties of PSs, their *in vivo* intermolecular interactions and the scope of designing newer formulations has widened their applications from conventional FLI to other advanced OI techniques like SERS imaging, UCL imaging (UCLI) and PAI. In this section, different OI modalities combined with PDT have been discussed separately.

Fluorescence Imaging Combined Photodynamic Therapy

FLI has become a highly adoptable clinical imaging modality for tumor detection to image-guided surgery [41]. Benefits of FLI involves: (a) high spatial resolution and sensitive investigation of both functional and structural changes, (b) non-invasive, safe technique using non-ionizing radiation, (c) making use of portable and low cost clinical equipments, (d) provide real-time images, (e) can be customized with microscopy and endoscopy to provide both microscopic and macroscopic information and (f) provide quantitative information for aimed diagnosis and follow-up [43]. However, the primary limitation of FLI is the poor penetration depth of light in biological tissues due to the scattering and absorption properties of tissue. Scattering results in loss of directionality of light, thus results in a blurred and low resolution images. Further the light absorbing endogenous molecules (melanin and hemoglobin) results in a reduction of light intensity, therefore significantly decreases the SNR in the visible range [44]. Thus, due to the drawbacks of autofluorescence signals and light scattering, the applications and designing of effective fluorescent agents remains a challenge. While the SNR can be improved by the use of long-lived fluorescent agents which can eliminate the short-lived background fluorescence interference during the imaging [45]. Owing to inherent optical absorption and fluorescence properties of PSs used in PDT, PSs offers their application as theranostic agents. In 1920s, Policard showed the first indication of PDT-related imaging via fluorescence with his observation that Hematoporphyrin (Hp) localization in tumor tissues was more fluorescent than normal ones in a rat sarcoma model. But it was only in the 1950s, Rasmussen-Taxdal and colleagues successfully proved the FLI technique clinically, by injecting Hp to patients prior to the excision of benign and malignant lesions [21].

Combined with its fluorescence property, preferential accumulation of PSs in neoplastic tissues has been shown to be inherently well-suited for selective fluorescence-based visualization of tumors to demarcate the boundaries of cancerous and healthy tissues, photodynamic diagnosis (PDD) and molecular imaging, an approach termed as PS fluorescence detection (PFD). PFD has been mainly applied for real-time imaging for FGS [46]. Currently, 3 PSs 5-aminolevulinic acid (5-ALA), methylene blue (MB) and indocyanine green (ICG), have been successfully applied clinically for FGS [47]. ALA and its derivative 5-ALA Hexylester (Hexvix®) have already approved for bladder cancer imaging.

Photofrin, a derivative of porphyrin has also been used for the detection of various malignant and premalignant tumors. Upon irradiation with a 405 nm full-color endoscopic FLI system, red fluorescence of Photofrin was shown to significantly overcome the green autofluorescence of tumor mass [48]. A single centre Phase III randomized controlled trial showed that ALA and Photofrin FGS and repetitive PDT offered a beneficial therapeutic advantage to patients with Glioblastoma multiforme without any risks [49]. Another promising randomized controlled multi-centre phase III trial evaluated the efficacy of ALA based FGS in enabling intraoperative visualization and resection of malignant glioma thus leading to an overall improvement in progression-free survival [50]. In a recent nonrandomized pilot study, a treatment regime including 5-ALA fluorescence-guided maximal resection followed by 5-ALA intraoperative PDT showed to be a good treatment option with prolonged survival in recurrent Glioblastoma multiforme patients [51].

Clinically, standard diagnostic imaging equipment such as endoscopes, laparoscopes, cystoscopes and neurosurgical microscopes are being implemented for FLI. Most of the PSs possess significantly high fluorescence quantum yield, which makes these PSs eligible candidates as dual-functional theranostic agents for clinical applications, however, Tookad is an exception. Although as most free forms of PSs lack sufficient biological stability, solubility and specificity, which has restricted the inclusion of only a few PSs into clinical applications as theranostic agents [21,22,47]. Compared to conventional imaging modalities such X-ray CT, MRI and PET, because of nonradioactive properties, fluorescence-based imaging is much safer and causes less damage in patients. However, due to the poor penetration depth of visible and NIR light of few millimeters in tissue, the FLI can only reach a limited depth as compared to nuclear imaging modalities [47]. Other than the limitation of in-depth penetration, as compared to the volume sensitive techniques like CT, MRI and PET, FLI is a surface-sensitive technique which cannot provide structural details during the process of resection, thus fails for tumor lesions with considerable subsurface depth [21,46]. To address these inherent limitations of PFD, extensive research is being focused on developing novel, more potent and tumor-specific PSs with potential clinical applications. In this regard, some of the approaches on PSs development, which are being explored includes: (1) enhancement of PS fluorescence, (2) novel PS with long excitation wavelength; (3) implementation of multimodal imaging approach based on PFD, complemented with depth-resolved

structural imaging modality. The recent progression of multifunctional platforms or delivery systems has also been explored for designing and delivery of PSs combining PFD with PDT. These multifunctional delivery systems also offer the advantage of efficient delivery of the hydrophobic PSs, to avoid reduction in their photodynamic efficacy due to self-aggregation and fluorescence quenching in aqueous media [46,52-54].

Although PS-based FGS has attracted a lot of attention and has created several opportunities in the surgical oncological field, still the chances of misdetection of sub-centimeter tumors are frequent. This usually results in the emergence of lethal recurrent cancers which are more difficult to treat. A recent approach in developing more selective PS-based OI is based on the incorporation of tumor-specific bio-responsive elements with PSs known as aPSs or photodynamic molecular beacons. These photodynamic molecular beacons remain non-fluorescent and non-cytotoxic due to the linked quencher with the PS. Under tumor specific conditions the linker gets cleaved resulting in release of free active PS with restored fluorescence emission and ROS generation property. Therefore, upon irradiation, aPS-based theranostic agents enable better and controlled tumor-selective PS fluorescence at microscopic level imaging along with selective destruction of disseminated, microscopic tumor mass through PDT and/or other modalities like resection [22,27,34,55]. Designing of photodynamic molecular beacons are based on three approaches: (1) aggregation-induced emission (AIE), (2) aggregation-induced quenching (AIQ) and (3) dual-labeled beacon [27,34]. AIE based PDT beacons are weakly or negligibly fluorescent in dissociated free state but exhibit intense fluorescence and strong photosensitization in the aggregate state due to the phenomena of restriction of intramolecular motions (RIM) [56,57]. While dual labeled PDT beacon is an advanced concept where the PS -quencher pair is conjugated with a tumor microenvironment bioresponsive linker molecule. Upon exposure to specific stimuli, disruptions of linker, lead to release of free PS regaining its fluorescence and ROS generation property [55,58].

The concept of PDT beacons dates back to 1982, when Moore et al., prepared carotenoporphyrin by joining a synthetic carotenoid to a tetraarylporphyrin through a flexible trimethylene linkage and showed that the carotenoid conjugation photo-protects the porphyrin and thus limit the nonspecific toxicity in biological systems [59]. Following this, other carotenoid analog conjugated PSs like meso-tetra-phenyl-substituted porphyrins, pheophorbide and

Hp were investigated as selective fluorescence-based tumor imaging and PDT agents [60–62]. However, this design failed to gain many applications due to the lack of selective separation and partial fluorescence quenching [63]. In 2004, Chen et al., reported the first proof-of-concept of aPS beacon where pyropheophorbide was conjugated to $^1\text{O}_2$ quencher carotenoid via a peptide linker, cleavable by a specific protease. Under *in vitro* condition this beacon also confirmed its selective activation upon targeting [64]. Other groups have also reported other self-quenched PS beacons covalently attached to carbon nanotubes, commercially available black hole quenchers (BHQs) and other carotenoids [58].

As compared to the self-quenched PDT beacon, AIE PSs exhibit enhanced fluorescence intensity which allows improved fluorescence-based self-tracking PS distribution in cellular systems during PDT. Moreover, these AIE PSs have persistent $^1\text{O}_2$ generation ability, which makes them potential candidates for efficacious fluorescence image-guided PDT. AIE PS theranostic molecular probes are designed with two main components: the AIE PS core, and the recognition element which is used to direct the *in vivo* PDT. Depending on the recognition groups the AIE PS molecular probes are classified as targetable and activatable. Designing of targetable AIE PS are based on the targetable ligand in tumor tissues where a choice of recognition element includes (i) hydrophilic targeting ligands such as biomarkers on the target cell surface; (ii) bioorthogonal labeling where the clickable groups are eventually interacting with the target cells via click reactions. Fluorescence and PDT activity of AIE PS is activated upon recognition interactions with the target ligand via the phenomena of RIM. While in the case of activatable AIE PS, the fluorescence and photosensitization property of PS is quenched by the tumor enzyme or stimuli-specific cleavable quenchers. Activatable elements provide improved selectivity of AIE PS molecular probes for imaging and therapy [57].

AIQ utilizes the concept of fluorescence quenching of PSs in aggregation state, thus keeps the fluorescence in the off state while circulation, and thereafter effectively regain their fluorescence upon disaggregation at the tumor site resulting into selective “off to on” fluorescence-based monitoring of tumors followed by PDT. The concept of AIQ based “off to on” fluorescence transduction has been demonstrated by Fu et al., where they reported a pH-responsive biodegradable and O_2 self-supplying Mn^{+2} doped calcium phosphate mineralized glucose oxidase nanoparticles (NPs) loaded with catalase and sinoporphyrin sodium as PS. This study demonstrates a novel concept of starvation therapy enhanced PDT

through the cascade reactions of glucose oxidase and catalase, whereby catalase catalyzes the decomposition of endogenous H_2O_2 to generate O_2 which promotes glucose oxidase to consume more intratumoral glucose. Furthermore, O_2 generation overcomes tumor hypoxia and improves PDT induced generation of $^1\text{O}_2$. These NPs showed selective accumulation at tumor sites monitored by FLI as well as Mn^{+2} mediated MRI [65]. In another study, Jiang et al., reported biocompatible polymeric NPs, pluronic F127 encapsulated hexyloxyethyl-devinyl pyropheophorbide-a (HPPH) and camptothecin (chemotherapeutic drug), whereby the NPs are selectively activated by ROS at the tumor site. Their “off-to-on” transition allowed tumor-selective FLI imaging along with synergetic chemo- and photodynamic treatment in *in vivo* xenograft tumor mice model [66].

Other approaches of designing activatable PDT beacons involve incorporation of multiple PSs to a polymeric carrier like chitosan, dextran, heparin, hyaluronic acid, glycol, polylysine, pullulan etc. Incorporation of PS in polymeric carriers results in efficient self-quenching of fluorescence quantum yield, thus nano-PS formulations remain photodynamically inactive during systemic circulation and activated only under tumor site specific molecular stimuli or environment conditions [58,67,68].

Over the decades, PS-based FLI-guided PDT and PDD had a long history of successful applications in clinical settings owing to high sensitivity, better spatial resolution, real-time and non-invasive mode of detection and visualization with already available instrumentations. However, due to off-target accumulation, activation, concentration and microenvironment-dependent fluorescence signal intensity of free PSs, limits their applications in real-time settings. These limitations of conventional PS have boosted the rapid advances in novel approaches and designing rationality for the development of next-generation PS-based FLI with the improved theranostic outcomes. A most feasible strategy that has been extensively explored includes the incorporation of PSs in nanostructures imparting the properties of targetability, uniform tumor tissue distribution, higher stability and longer circulation time. Herein designing strategy based on assembly-driven molecular beacons and aggregations has been discussed as potential fluorescent imaging probes. The major importance of assembly-based PS design is that the photophysical properties of PS can be conveniently regulated by controlling their assembly arrangements. Furthermore, advances in imaging systems, and image analysis algorithms has

also revolutionized the field of FLI-guided PDT. However, even after possessing many advantages most clinically and non-clinically used PSs are responsive to light of wavelength region 630 -700 nm with poor tissues penetration and their fluorescence properties vary considerably with a change in microenvironments, limiting the FLI resolution and sensitivity. Thus, the inherent limitations of visible region bioimaging have uplifted the research areas of new OI techniques in PDT such as PAI, SERS and UCLI, due to their unique strengths making them suitable for high-precision and resolution bioimaging.

Photoacoustic Imaging Combined Photodynamic Therapy

PAI (also referred as optoacoustic) is a rapidly emerging promising non-ionizing, non-invasive technique of biomedical imaging modality providing simultaneous *in vivo* structural, functional and molecular information at clinically relevant penetration depths. As compared to existing imaging techniques, PAI being a hybrid imaging method provides high spatial resolution and image contrast by combining the advantages of both OI (contrast quality, spectral sensitivity) and US imaging (in-depth tissue penetration, high resolution) [69,70]. During PAI, absorption of light energy by endogenous chromophores (e.g., hemoglobin and melanin) present in tissues, results in their rapid thermoelastic expansion, generating wide-band photoacoustic (PA) transients or US waves. US transducers detect the generated US waves at the external surface of the tissue by converting the mechanical US waves to electrical signals which are further processed to form an image. Compared to conventional OI modality, PAI enables imaging at a greater penetration depth of tissues (5–6 cm), thus allows deep tissue imaging in clinics [70–72]. PAI enables the imaging of dense and unorganized vasculature in malignant tumors due to the higher concentration of hemoglobin and melanin in tumor mass/vasculature compared with normal tissue. PAI have been reported to detect tumor vascular networks in the rat brain, the blood-oxygenation dynamics in the mouse brain, human arm, as well as breast cancer imaging based on endogenous chromophores [70]. Additionally, utilization of PA exogenous contrast agents such as NIR-absorbing dyes (ICG, IRDye800CW and AlexaFluor 750), carbon nanotubes as well as gold NPs can significantly enhance the sensitivity and contrast of the PAI in deeply situated tumors [73,74]. However, cytotoxicity issues and low blood circulation time of these exogenous contrast agents limit their clinical application [70,71]. This necessitates the use of some biologically compatible agents with

minimum side effects. In this regard Ho and colleagues evaluated five different PSs with low fluorescence quantum yields, zinc phthalocyanine (ZnPc), protoporphyrin IX (PpIX), 2,4-bis[4-(N,N-dibenzylamino)-2,6-dihydroxyphenyl] squaraine (Sq), chlorin e6 (Ce6) and MB as potential PA contrast agents in a phantom model. Among all the tested PSs, ZnPc showed the highest PA activity. Subsequent *in vivo* studies showed preferential accumulation of ZnPc in tumors which was evident from PAI of its localization and biodistribution thus enabling to achieve longitudinal monitoring of cancer. Thus, these PS-based PA contrast agents can offer great potential in PAI based cancer diagnosis combined with PDT. PSs with low fluorescence quantum yields usually possess high PA activity, due to the fact that an excited molecule can relax back to the ground state either through fluorescence emission or thermally through internal conversion [70]. PS molecules can provide the advantage of combining FLI and PAI. Both imaging techniques provide a number of complementary advantages, FLI can gain sensitivity at single molecule level at superficial depth, while PAI accomplish significantly better deep tissue spatial resolution together with non-interference from photobleaching and autofluorescence issues [75]. In another study, Abuteen et al., evaluated six free base tetrapyrrolic PSs of two different classes (quinoline-annulated porphyrins and bacteriochlorins) with NIR absorption, low fluorescence emission and $^1\text{O}_2$ quantum yields for their PA contrast generating efficiency with respect to standard PA contrast agent ICG. The study demonstrated that these tetrapyrroles allow PAI of a sub-mm target up to 2 cm depth in tissue mimicking phantom, thus suggesting the use of these PSs as potential exogenous PAI contrast agents to be evaluated for *in vivo* studies [76]. Similarly, Attia and colleagues investigated the biodistribution and fate of the phthalocyanines in the biological tissues by studying the PA activity of three water-soluble phthalocyanines: phthalocyanine tetrasulfonic acid (PcS4), Zn(II) phthalocyanine tetrasulfonic acid (ZnPcS4) and Al(III) phthalocyanine chloride tetrasulfonic acid (AlPcS4) in phantom and mice bearing oral squamous cell carcinoma xenograft. Among all the three phthalocyanines, PcS4 conferred the highest PA activity in both phantom and tumoral mice, showing the highest accumulation in the tumor at 1 h post-injection, suggesting PcS4 as a promising PA contrast agent and can be successfully exploited as a photodiagnostic agent [77].

Other than free base PS, many metallated and non-metallated PS-based nanoformulations have also been investigated as promising PAI agents. The optical absorption coefficient of a free base PS has

shown to be not sufficient to obtain a significant SNR for *in vivo* PAI, because PA signal generation is mainly dependent on the optical absorption properties of the structure being imaged. Nanosystems with encapsulated PS molecules can provide enhanced PA contrast by quenching the fluorescence quantum yield of the closely spaced PS molecules [11]. For example, MacDonald et al., showed that relative to free-base porphyrins, Mn-porphyrin-phospholipid provides enhanced PA signals with PAI in phantoms. This increase in PA signals is attributed due to a drastic decrease in PS excited-state lifetimes because of insertion of paramagnetic Mn²⁺ ions into porphyrins, thus directing the PS excited states into nonradiative decay paths and acts purely in the photothermal mode producing PA waves [78]. Another porphyrin-lipid shell microbubbles (MBs), termed "porphyrin MBs", were reported by Huynh and collaborators and were investigated for PA properties in tumor xenograft mice model. The dense packing of porphyrins within the shell of MBs displays very high optical absorption properties, generating strong PA signals, which was evident from the enhanced PA signals in tumor mass, post porphyrin MBs injections [79,80]. A lipid-conjugated Zn-chlorin derivative was used to synthesize Zn-MeO-chlorin lipid nanovesicles which showed PA contrast enhancement with narrow NIR absorption band, which showed favorable spectral un-mixing within the biological light absorbing and scattering environment a hamster oral carcinoma model, thus proving its potential as contrast agents for PAI [81]. Another study showed that due to endogenous light absorption by hemoglobin, only large blood vessels could be visualized in the tumor mice model upon PAI. However, enhancement of PA signal in the whole tumor mass occurred post injection of IR825@C18PMH-PEG-Ce6-Gd micelles, showing accumulation of these NPs in tumor tissue, thus allowing PAI-guided PDT [82]. Similarly, PA image contrasting ability of the hypoxia-activated prodrug formulation AQ4N-hCe6-liposome was evaluated in tumor-bearing mice. PAI results indicated that mice those were intravenously injected with AQ4N-hCe6-liposome showed ~2.5 times increased PA signals in tumors than others without AQ4N-hCe6-liposome injection [83].

Furthermore, metallic plasmonic NPs exhibits several fold higher absorption coefficients compared to endogenous chromophores, making them favorable for PAI based monitoring for their tumoral uptake studies [11]. As an example, Ce6 -loaded plasmonic vesicular assemblies of gold nanoparticles (AuNPs) reported by Lin et al., showed improved tumoral uptake of PS following heat-induced release of the

Ce6 cargo along with *in vivo* PAI combined PDT potential [84]. Similarly, Ding et al., described the synthesis of nanocrystallite ZnPc nanodots (ZnPcNDs), by cryodesiccation-driven crystallization approach, which was further surface modified with Pluronic F127 and folic acid (FA), endowing them with good water solubility and stealth properties in blood, which allows them to avoid immunological detection and destruction thus prolonging their circulation time. These nanodots showed efficient cancer cell targeting, for simultaneous PAI and PDT [85]. Also, ultra-small pyropheophorbide-a-PEG nanodots were reported for PAI/FLI-guided PDT with effective renal clearance properties without any long-term side effects [86]. PS sinoporphyrin sodium loaded PEGylated graphene oxide reported by Yan et al., also exhibited great potential for enhanced FL/PA dual-modal imaging-guided synergistic PDT and photothermal therapy (PTT) in human adenocarcinoma mice model [87]. Many other nanoformulations loaded with suitable PSs have been explored for PDT combined PAI theranostic agents [11].

Although PAI technology dates back to 1980s, however its being in recent years only that PAI have been explored extensively for its potential in optimizing PDT outcome by providing scalable and multi-contrast images with 3D real-time feedback. PAI not only provides information about biodistribution, pharmacokinetics and uptake of PS in tumor mass for image-guided PDT but have also been utilized for monitoring real-time vascular destruction and changes in tissue O₂ levels post-PDT, thus allows optimization of PDT dose parameters. One of the important aspects is that even PSs with poor fluorescence quantum yield which are generally not suitable for FLI can be successfully utilized for PAI. As discussed, designing of nano assemblies of PSs leads to novel approaches of highly spatiotemporal and non-invasive combination of FLI and PAI. However, various instrumental and biological conditions limit PAI's performance in the clinical set-up which includes (1) limited aperture and finite size and shape of US transducer results into "limited-view" condition, (2) narrow detection bandwidth of transducer compared to a wide frequency range of PA signals generated from the sample surface causes bandwidth mismatching, (3) a part of optical and acoustic attenuation effects in tissues also results in a poor spatial resolution which further decreases with depth and (4) tissue heterogeneity cause a complex speed-of-sound distribution that complicates image reconstruction [88]. Thus, utilizing PS nanoconstructs for PAI holds great promise into clinical translations provided that

the limitations of instruments and image reconstruction algorithms need to be addressed.

Upconversion Luminescence Imaging Combined Photodynamic Therapy

In recent years, UCL has gained notable attention in the field of cancer therapy and imaging over conventional luminescence techniques (organic dyes and quantum dots). In principle, UCL is an optical process and make use of lanthanide ions (Yb^{3+} , Er^{3+} , and Tm^{3+}) based upconversion nanoparticles (UCNPs) which are excited by low-energy radiation (NIR light) to generate higher energy emission (visible or UV light) caused by an anti-stokes mechanism (Figure 6A). In comparison to conventional light responsive fluorescent imaging agents, UCNPs possess many unique properties of high conversion efficiency and light penetration in biological tissues such as photostability, long lifetime, non-photobleaching, narrow emission peaks, large stokes shifts and low toxicity. Moreover, the use of low energy radiation reduces light induced unwanted cellular damage and offers the advantages of very low auto-fluorescence and high detection sensitivity. All these advantages widened the application of UCNPs from therapy to *in vivo* imaging [89]. UCNPs have already been utilized to overcome the limitation of visible light excitation of traditional PSs, which suffers from low penetration depth in tissue to achieve NIR-triggered PDT. Majorly, lanthanide-doped UCNPs have shown to accomplish NIR-triggered PDT. As illustrated in Figure 6A, upon excitation by NIR, UCNPs efficiently convert the deeply penetrating NIR into visible wavelength light which eventually excites the UCNP conjugated or encapsulated PSs, bestowing the essential advantage of PDT of deep-seated tumors. Furthermore, excitation of UCNPs with NIR light results in release of photons of both higher wavelength (red) and shorter wavelength (green), which makes them a potential candidate for simultaneous PDT and *in vivo* OI or more specifically UCLI-guided PDT (Figure 6B) [89–92]. For example, Park et al., reported the synthesis of Ce6 conjugated $\text{NaYF}_4:\text{Yb},\text{Er}/\text{NaGdF}_4$ core-shell, which showed accumulation in tumor tissues by the enhanced permeability and retention (EPR) effect in the tumoral mice model. Upon excitation with a 980 nm laser, UCNPs showed both red and green emission, used to visualize tumors with UCLI and also demonstrated efficacious PDT outcomes [93]. Similarly, excitation of $\text{MC540-AuNR@UCNP@NBUC}$ with 808 nm laser allowed high-resolution UCLI of tumors by upconverted green and red lights at 520 nm and 654 nm along with AuNR@UCNP energy transfer

mediated PDT by Merocyanine 540 [94].

Another bioresponsive FeOOH modified and toluidine blue (TB)-loaded $\text{NaLuF}_4:\text{Yb},\text{Er},\text{Tm}@ \text{NaLuF}_4$ (RE-FeOOH-TB) nanoformulation was reported for UCLI-guided PDT for *in vivo* tumor model. In response to intratumoral acidity and reducibility, FeOOH reacts and quenches GSH, subsequently releasing Fe^{2+} and catalyzing H_2O_2 to produce O_2 , which improves intratumoral dissolved O_2 for PDT. Upon NIR excitation, UCNPs emits 800 nm mediated UCLI and 650 nm for excitation of TB for PDT [95]. Similarly, many other PS conjugated UCNPs, such as hyaluronate fullerene conjugated 3-aminophenylboronic acid functionalized UCNPs, ZnPc conjugated spindle $\text{UCNP@SiO}_2@\text{AuNPs}$, trimethylpyridylporphyrin-fullerene (PC70) decorated FA/PEG-coated $\text{NaGdF}_4:\text{Yb},\text{Tm}@ \text{NaGdF}_4$, ZnPc conjugated $\text{NaYF}_4:\text{Er}@ \text{NaXF}_4$, AIPcS_4 -conjugated PEG-coated $\text{Fe}_3\text{O}_4@\text{NaYF}_4:\text{Yb}/\text{Er}$ have been shown to exhibit promising PDT efficacy combined with UCLI [96–100]. Recently Feng et al., introduced proof of concept to realize PDT “off” and “on” switching, to overcome the damage to normal cells and the photosensitivity to the skin during imaging/diagnosis by making use of bioorthogonal chemistry. They utilized UCNPs anchored with one handle of click reaction tetrazine (Tz) and targeting entity to form UCNPs-Tz/FAPEG. UCL images of tumor region were recorded after intravenous (i.v.) injection of the UCNPs-Tz/FAPEG upon exposure to 980 nm laser light which showed their selective accumulation in tumor tissue due to FA targeting and EPR effect. Upon selective accumulation, *in situ* injections of the other handle of the bioorthogonal reaction, Rose Bengal (RB) conjugated norbornylene (NB), allowed click reaction between Tz and NB to efficiently link the PS to the UCNPs. This further enabled highly effective PDT in tumor-bearing mice via effective energy transfer between UCNP and the RB [101].

Owing to several advantages of UCNPs, UCLI is being considered as an upgraded alternative to traditional OI-guided tumor therapy more importantly for their ability in long-term repetitive FLI and effective penetration depth in deep-seated tumor by NIR excitation. Furthermore, UCNP acts as suitable tumor-selective drug delivery carriers for hydrophobic PSs along with activating PSs in deep-seated tumors for effective PDT. Further, as wavelengths of > 800 nm are used for UCNP-PS excitation, this is advantageous over the use of free PS molecules. Far-red wavelength of 800 nm cannot be used for excitation of free PS, as the photons of wavelengths of ≥ 800 nm do not provide enough energy to excite O_2 to $^1\text{O}_2$ state. Another interesting feature is the utilization of the same lanthanide doped

UCNPs for multimodal imaging capabilities for example NaGdF₄ for MRI and UCLI; NaLuF₄ for CT and UCLI and radionuclide UCNPs for UCLI combined PET/SPECT. Moreover, PA contrast agents absorbing in NIR region causes an increase in the PA signal thus UCNPs can also be effectively exploited for dual PAI and UCLI. Although NIR have deep penetration in tissues, however considering the fact that the emitted UCL must be detected outside the imaging object, UCLI penetration depth was reported to be only ~3.2 cm upon 980 nm excitation [102]. Besides this, certain other caveats include (1) NIR excitations (~ 980 nm) generates non-negligible heating of the exposed tissues and also cause light attenuation due to overlap with water absorption; and (2) narrow excitation bands and low absorption cross-sections of UCNPs together with surface quenching effects reduce UCL brightness [103]. Further, the practical applications and designing of UCNPs for UCL guided PDT impose several challenges majorly in their designs such as their composition, size, surface functionalization, physiological stability, PS loading, upconversion efficiency and absorption spectra overlap of UCL-PS pair [91]. Thus, multidisciplinary efforts need to be

addressed for establishing this synergistic combination of UCNP and PSs to augment the scope of improved PDT and imaging in near future.

Surface-Enhanced Raman Scattering Imaging Combined Photodynamic Therapy

In past few years, SERS imaging with biocompatible SERS probes have emerged as a novel *in vivo* cancer imaging technique. SERS is a phenomenon in which the Raman intensity of a molecule is enhanced enormously (up to 10¹⁴-fold) when placed near a noble metal surface such as silver or gold NPs. SERS imaging holds great potential over other imaging methods in the field of medical imaging as the SERS nanoprobe has enhanced photostability, high sensitivity, higher signal specificity and multiplexing capabilities [104]. As illustrated in Figure 7, the principle of SERS imaging is based on electronic transitions of both Rayleigh and Raman scattered photons by SERS probe, further having frequency and wavelength different from the incident photons. SERS imaging has also proved to be efficient in the detection of circulating tumor cells and multiplex tumor-associated cell surface antigens and can be used to visualize tumor margins allowing

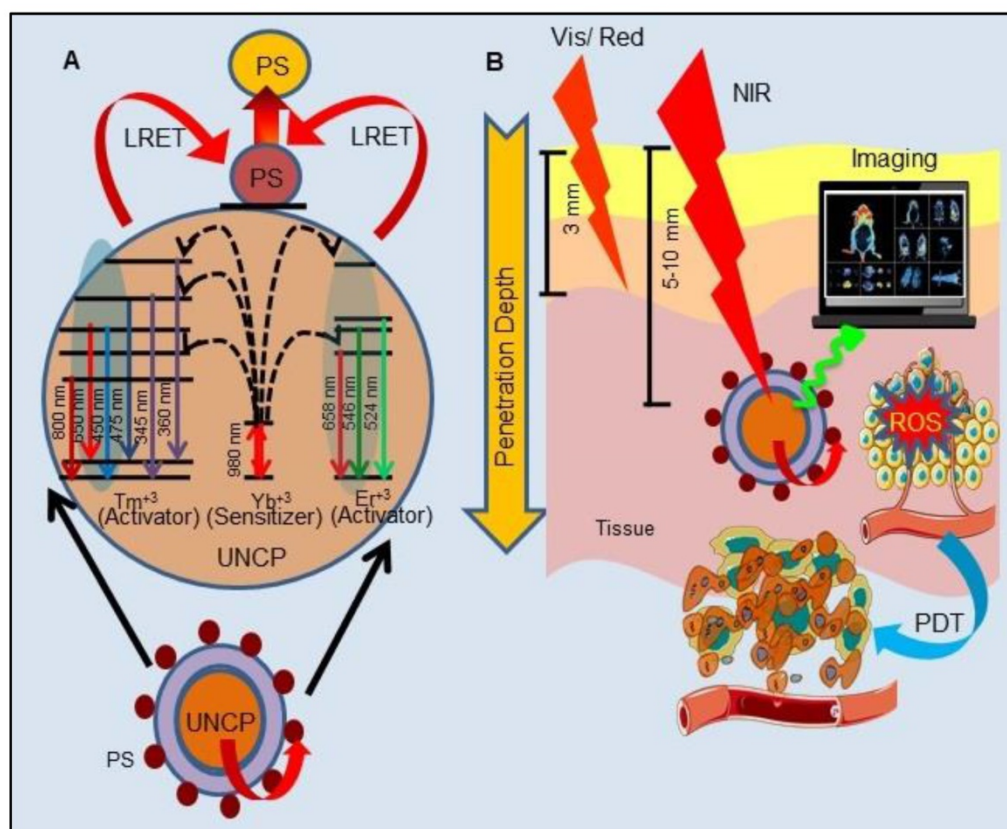


Figure 6. Schematic illustration of principle of upconverting nanoparticles (UCNPs) mediated Upconversion Luminescence (UCL) imaging and Photodynamic Therapy (PDT): **A.** Upconversion process in the UCNPs under Near Infrared Radiation (NIR) excitation, and the Luminescence resonance energy transfer (LRET) between UCNP and photosensitizer (PS). **B.** Deeper penetration of NIR compared to visible light excites UCNPs and converts NIR to visible wavelength emission for activation of the PS producing Reactive Oxygen Species (ROS) to induce PDT mediated tumor damage with simultaneous imaging with UCL.

guided tumor resection [105]. Interaction of photoactive molecules, porphyrins with metallic nanostructures imparts several important properties which include charge transfer, plasmon-enhanced electrical conduction and electrocatalytic activity. The heterocyclic pyrrole structure of porphyrins contributes to its strong Raman scattering properties, and which can be conveniently enhanced by both electromagnetic and charge transfer to exhibit SERS spectra. Further the absorption spectra of porphyrins have significant overlap with the plasmon band of AgNPs and forms charge-transfer complex with AgNPs, thus making porphyrins potential SERS imaging agents combined with PDT. As an example, the complexation of tetra(4-aminophenyl) porphyrin with AgNPs shown to undergo charge-transfer complexation in the ground state, which was confirmed by red-shifted ground-state absorption and SERS property [106]. Interestingly, Zhang et al., reported the interaction of RB with silver island films (SiFs) caused a three-fold increase in $^1\text{O}_2$ generation due to the enhanced triplet excited state yield of the PS, a phenomenon known as Metal-Enhanced $^1\text{O}_2$ generation resulting from the interactions between plasmons and photoactive molecules [107]. Similarly, many other PSs such as 5-ALA, PpIX, conjugated on AuNP surface significantly enhanced the PDT efficacy in cancer cells which is attributed to the enhancement in ROS generation by PS due to highly localized plasmonic field of the AuNPs [108,109]. These findings formed the basis for the development of novel theranostic systems for SERS imaging-guided real-time monitoring of PDT. In most of the reported studies, AuNPs have been widely used as SERS imaging probes and photothermal agents due to their enhanced SERS effect and high photothermal conversion efficiency [105,110–113]. While very few studies have involved SERS-PS probes for PDT combined SERS imaging. One such example involves FA receptor mediated SERS imaging, based on the utilization of nanodrug PpIX-GNR-MBA-FA. Where, PS PpIX function in SERS imaging, mecaptobenzoic acid (MBA) as Raman reporter molecule and Gold nanorods (GNR) mediates photothermal conversion and enhanced PDT efficiency [114]. Other studies include multilayer-coated AuNPs where PSs (PpIX, MB) were loaded in silica and polymer layers, they showed potential for simultaneous SERS-based tumor detection and PDT in the tumoral model [115,116]. Zheng et al., demonstrated a novel strategy to construct SERS probes by utilizing a non-fluorescent Mn-porphyrin-phospholipid conjugate (MnPL) to serve as both the Raman dye and a stabilizing

biocompatible surface coating agent on AuNPs [117]. Further, they coated AuNPs with other non-fluorescent Pd-porphyrinoids forming PdPL-NPs where coupling with plasmonic NPs imparted both SERS mediated reporting and monitoring capability. Interaction between plasmonic metallic NPs with fluorescently inactive PSs allow for the decoupling of the therapeutic and imaging mechanisms so that both phenomena can be optimized independently. This phenomenon allows for *in vivo* tracking of non-fluorescent PSs which is otherwise not possible with conventional FLI along with overcoming its limitation of background autofluorescence. Most importantly, this design allowed the excitation of PdPL-NPs with the same laser wavelength (638 nm) to stimulate them both as SERS reporters and photosensitizing agents. This provides the advantage of real-time SERS-based dosimetry for monitoring PS concentration at the tumor site and PDT dose delivery. Moreover, nano-enabled SERS reporting PSs uses entirely different physical mechanisms of absorption by PSs and scattering by AuNPs, resulting in the mutually exclusive output of enhanced PDT and SERS signals [118].

Although the results obtained with PS based SERS reporter agents are fascinating, still this research is at the basic stage and more in-depth understanding of the underlying mechanism(s) governing the change in SERS intensity in relation to the PDT dose and other more efficient designs needs to be explored. In general, the designing of SERS nanoparticles is based on certain logical approaches: (1) the selected metallic material should have high SERS enhancement, which restricts the utilization of only three best-known SERS materials Au, Ag and Cu, (2) encapsulation of SERS nanoparticles to protect and isolate the Raman active material from surrounding *in vivo* conditions which is most important to preserve the unique identifying Raman fingerprint and retain its detection ability [119]. Despite the advantages of SERS imaging, other than rationale designing of SERS, many additional technical obstacles need to be addressed before its clinical deployment. Effort needs to be taken for developing more advanced Raman detectors with a wide field of view, rapid image acquisition speeds and deep tissue imaging ability as the presently available Raman scanners lack all of these. Further, development of more robust imaging algorithms are required to detect very fine spectral differences between cancerous and non-cancerous cells, which usually goes undetectable in direct analysis of the Raman spectra.

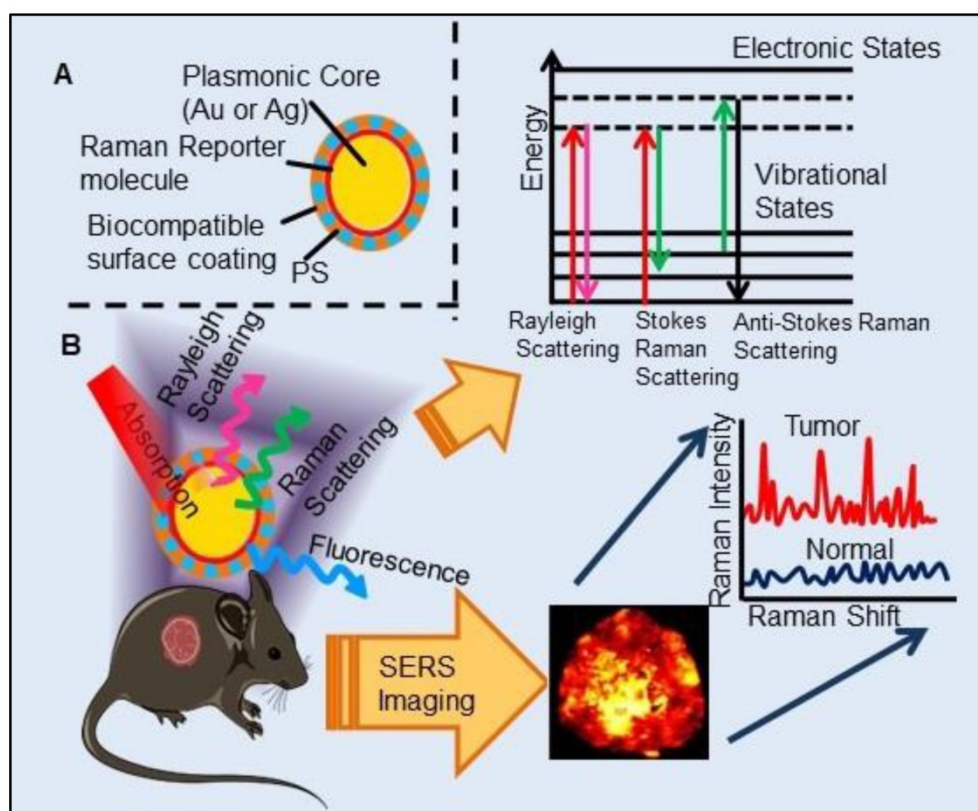


Figure 7. Schematic design and illustration of Surface-Enhanced Raman Scattering (SERS) probes for *in vivo* imaging: **A.** Structure of SERS probe consisting of a metal nanoparticle as plasmonic core, adsorbed Raman reporter molecule on the metal surface, a biocompatible surface coating layer loaded with photosensitizer (PS). **B.** Depiction of energy transitions of photons during different types of light scattering upon absorption of light by plasmonic nanoparticle. Representation of SERS image and SERS spectra of tumor.

Magnetic Resonance Imaging combined Photodynamic Therapy

Since its first application, MRI has become one of the powerful, non-invasive technologies for soft tissue imaging in clinics, among all the available oncological diagnostic methods. It enables 3D anatomical imaging combined with high spatio-temporal resolution thus provides the ability to track physiological and molecular events. The contrast generated due to magnetic resonance (MR) signal occurs due to differences in relaxation times of water protons (T1 and T2) and/or the proton density of water molecules in different soft tissues. These differences in proton behaviors allow tissue discrimination [120]. Although in most of the cases, the contrast generated due to indigenous tissues protons between healthy and diseased tissues are too weak to be imaged which necessitates the use of external contrast agents. These contrast agents generally enhance the relaxation behaviors of interacting water protons in its vicinity, thus improving the overall MRI image contrast. MRI contrast agents are either paramagnetic ion complexes or superparamagnetic magnetite particles (iron oxide nanoparticles, SPIONs), which are being used for cancer detection and diagnosis. Paramagnetic

complexes containing manganese (Mn^{2+}) or gadolinium (Gd^{3+}) tends to reduce both T1 and T2 relaxation times, while SPION contrast agents shorten the T2 and T2* relaxation times of the residing tissues. Based on the differences in generated MRI weighted images, paramagnetic and SPION contrast agents are known as positive and negative contrast agents, respectively [121]. Gd(III)-based chelation complexes such as GdDOTA (DOTA = 1,4,7,10-tetraazacyclododecane-1,4,7,10-tetraacetate), GdDTPA (DTPA = diethylenetriamine pentaacetate) are routinely used in clinics [121]. MRI has already shown its promising applications in the detection of solid tumors for image-guided local destruction of cancerous tissues by various therapies like radiotherapy, radiofrequency (RF) ablation, thermoablation, cryoablation, and laser ablation. Similarly, contrast-enhanced MRI-guided PDT, has been explored successfully for precise detection of interstitial lesions and guide local light irradiation to maximize the therapeutic efficacy [122]. Further, studies have shown that PDT-induced changes alter proton behaviors in the tumor tissue and such changes can be enhanced using MRI contrast agents. Thus, MRI-guided PDT allows the determination of treatment parameters like PS concentration, light dose

in relation to the final treatment outcome [32].

Administration of Gd-based MRI contrast agents post-PS injection and PDT have already been shown to provide various sensitive information for the assessment of treatment outcome along with direct visualization of vascular damage for *in vivo* MRI-guided PDT in humans [21,32]. Although administration of contrast agent and PS as separate entities imparts the limitation of different pharmacodynamics and pharmacokinetics of two agents, resulting in differences in their biodistribution-based imaging. Incorporating a MRI contrast agent and a PS in a single theranostic agent has shown to overcome this limitation where the contrast agent and PS having the same biodistribution patterns further optimize the PDT treatment. Moreover, such a strategy of combining bimodal agents within a single molecular entity provides with the further advantages of increased hydrophilicity of PS in biological fluids and improved proton relaxivity for MRI efficacy due to the increased molecular weight [120]. Moreover, increasing interest in designing an efficient PS based contrast agents lies in the fact that till date no commercially available contrast agents are efficient enough for effective detection of malignant neoplastic tissues. Designing of potential contrast agents are based on various crucial factors like kinetic and thermodynamic stability, binding efficiency of water molecules with the complex, its exchange rate with the bulk water system, strength of the magnetic field, effect of temperature, and concentration [37]. Different approaches for developing MRI-PDT theranostic agents involve PS-MRI contrast agent as conjugated complexes, paramagnetic metallo-PSs and nanoformulations of contrast agent and PS. Although most of these PS based contrast agents have not been explored for their PDT ability, still these bi/multifunctional complexes have the potential for combined MRI and PDT applications.

Paramagnetic Metallated Photosensitizers

Paramagnetic metallo-PSs are the most extensively explored approaches for designing contrast agents. Incorporation of paramagnetic metals within tetrapyrrole rings of porphyrins along with appropriate side groups have been shown to enhance the relaxivity of surrounding water molecules thus generating MR contrast. Further, these complexes have a lesser possibility for release of metal ions from the porphyrin structure during systemic circulation and tissue accumulations due to their kinetic inertness, which lowers the risk of systemic toxicity induced by Gd and Mn ions [37]. The potency of metallated tetrapyrrolic-based macrocycles were

explored as MRI contrast agents for the first time in 1984. First PS based contrast agents were based on Cu(II), Fe(III), and Mn(III) inserted meso-tetrasulphonated phenyl porphyrin (TPPS4). Among these metallo-TPPS4 complexes, Mn(III)-TSPP4 was shown to be the best MRI contrast agent, followed by Fe(III)-TSPP4, while Cu(II) complexed TSPP4 showed the least MRI contrast [123]. In 1984, Furmanski et al. demonstrated the paramagnetic metalloporphyrins as tumor-selective MRI contrast agents for *in vivo* imaging of human tumor xenografts in nude mice [124]. Among all other metallated-PS complexes, Mn-meso-sulfonatophenyl porphyrins have drawn attention as potential MRI contrast agents with a variety of different formulations, designs or functional groups and investigated in various *in vivo* animal cancer models [125–127]. Another study reported that a water-soluble C60-Mn porphyrin exhibited improved water protons relaxation in comparison to free Mn-porphyrins due to the introduction of fullerene derivatives to Mn(III) porphyrins [128]. Furthermore, Mn-porphyrin complex has also been studied as partial oxygen pressure (pO₂)-responsive MRI contrast agents based on the redox switching of Mn(II/III)-porphyrin complexes [129].

Besides transition metals, porphyrin cavity can also accommodate lanthanide ions, which are of potential interest in a range of diagnostic and therapeutic medical applications. Due to the large size of Gd⁺³ ions, it cannot get accommodated in the macrocyclic center of common porphyrins, hence a new class of expanded porphyrins known as texaphyrins were used to synthesize Gd(III)- PS complex [130]. Sessler et al., synthesized and investigated a water-soluble, stable and non-toxic Gd(III)-texaphyrin/ Motexafin gadolinium (MGd) as a promising *in vivo* MRI contrast agent capable of targeting the liver and useful for detecting cancers, with 3–4 times greater relaxivity than the conventional MRI contrast agents can generate [131,132]. Although, Gd(III)-texaphyrin intensively studied for cancer PDT or radio-therapy from preclinical to clinical trials, however, it raised concerns due to disappointing results and controversies about the reproducibility of studies [130]. Similarly, two porphyrazine macrocycles complexes chelated with central Gd⁺³ cation, were reported as multifunctional agents for MRI and FLI-guided PDT [133].

Photosensitizer-MRI Contrast Agent Conjugates

Another approach of developing tumor-avid MR contrast agent involves conjugation of already available MRI contrast agents with the tetrapyrrole

structure of PS as functional side groups. Such PS-MRI contrast agent conjugates provide several advantages such as (1) increased relaxivity of contrast agent due to the increased size of the conjugates, promotes better proton exchange property along with reducing the tumbling rate of the molecule; (2) hydrophilic contrast agent confers amphipathicity to the conjugates, helps in increasing the water solubility of hydrophobic PS and promotes accumulation in the tumor site [134]. One of the first such examples is bis-Gd-DTPA-mesoporphyrin (Gd-MP or Gadophrin-2), where two Gd-DTPA moieties have been covalently linked to mesoporphyrin as side chains [135]. Later, Gadophrin-2 was modified into Gadophrin-3 by inserting a copper at the porphyrin core of Gadophrin-2 which improved the stability and safety of the complex [130,136]. Upon MR imaging, both the complexes showed greater accumulation in necrotic tumor regions in comparison to viable tumor tissue in xenograft tumor mouse models [135,137]. Moreover, Gadophrin-2 was studied as a bifunctional contrast agent for *in vitro* cell labeling and *in vivo* tracking of transplanted stem cells using fluorescence microscopy, OI and MRI [138]. In some porphyrin-paramagnetic ion/complexes, chelation has been carried out at both core and side groups to improve proton relaxation efficacy, for instance Mn-methylpyrroloporphyrin-gadopentetate di-meglumine (Mn-MPP-Gd-DTPA) [130,139]. The core structure of 5,10,15,20-tetraphenylporphyrin (TPP) was linked to one and four GdDTPA complexes through amide bond formation as side chains, which showed better MR relaxivity, compared to that of the widely used Gd-DTPA [140]. In an effort to combine two or more different diagnostic imaging techniques, Gros et al., synthesized a series of water-soluble bi/multimodal heterobimetallic contrast agents, where MRI agents like gadolinium polyamino-polyacetates (Gd(DO3A-AM) and [Gd(DOTA)(H2O)]) are linked as side chains on a Cu-porphyrin. These heterobimetallic Gd(III)/ Cu(II) complexes imparts MRI contrast by Gd(III) agents, while, PET, OI and FLI due to ⁶⁴Cu-porphyrin [141,142]. In another study, Zn(II) and Cu(II) porphyrazine (Pz) have been linked to GdDO3A-amide analogs, where Cu-Pz-Gd(III) complex exhibited the highest relaxivity, better cellular internalization and MR contrast enhancement, representing necrosis both *in vitro* and *in vivo* [143]. Designing of PS-MRI contrast agent conjugates is mainly focused on the use of Gd(III) ions due to the superior paramagnetic character of Gd³⁺ ions. Thus, researchers prefer to obtain Gd-PS based MRI agents by covalently linking Gd-MRI chelates at the periphery of tetrapyrrolic macrocyclic core [36].

Several PS-contrast agent conjugates have been

explored as multimodal theranostic agents for combined diagnostic imaging (MRI and FLI) and PDT applications [36]. Although utilization of tetrapyrroles as tumor avid MRI contrast agent has been started early, however, applications of these complexes as bi/multimodal theranostic agents were investigated lately. In 1993, Hindré et al., studied a series of Gd(III)DTPA conjugated TPP, which showed promising results for both MRI and PDT in nude mice [144]. This was reported to be the first prototype used for combined MRI-PDT theranostic applications. Later in 2000, Pandey et al., extensively investigated a new family of bifunctional theranostic agents combining two modalities into a single cost-effective “see and treat” approach, i.e., a single agent that can be used for contrast agent-enhanced MR and FLI followed by targeted PDT [145,146]. Investigated agents were based on a chlorophyll-a derivative HPPH, conjugated with one, two, three, or six GdDTPA. HPPH-3GdDTPA was reported to be the best candidate with respect to its imaging and PDT efficacy [32]. Similarly, phthalocyanine and porphyrazine - Gd(III) contrast agent conjugates also showed promising results for cancer imaging with both MRI and NIR fluorescence, along with effective phototoxicity [147,148]. In an effort to integrate chemotherapeutics and PDT along with MRI, Wu et al., synthesized tetraplatinated porphyrin Gd(III) complexes (Gd/Pt-Porphyrin) which was simultaneously conjugated with cisplatin at the side groups and Gd(III) to the central cavity of tetra-(4-pyridyl) porphyrin. Herein, the platinum component in Gd/Pt-Porphyrin induced chemotherapy while the Gd(III)-porphyrin complex played dual roles as MR imaging and PDT agent [149]. Ventura et al., synthesized conjugates with four [GdDTTA] linked to a meso-TPP core, as well as its yttrium(III) analog, as potential theranostic agents for MRI and one photon PDT. Further, Ventura et al., reported a series of conjugates with diketopyrrolo-pyrrole-Zn(II) porphyrinic core linked to a varied number of GdDOTA moieties; DPP-ZnP-GdDOTA, DPP-ZnP-(GdDOTA)₂ and GdDOTA-ZnP-ZnP-GdDOTA. These conjugates exhibited good ¹O₂ generation ability with high NIR two-photon PDT in cancer cells with remarkable fluorescence and MR imaging property. Two-photon PDT involves excitation of PS at the NIR region, which allows deep tissue treatment with minimal photodamage to surrounding healthy tissues. Further, two-photon irradiation can achieve high spatial treatment precision due to its application in a very restricted area [134,150,151].

Photosensitizer-conjugated MRI Nanoparticles

Recently to overcome the limitations of solubility and stability of PSs in blood circulation, photosensitizing NPs has emerged as a better therapeutic strategy to improve PS tumor targeting. Moreover, encapsulation of PSs in NPs allows for multi-modal/functional PDT-based synergistic therapeutic and diagnostic applications with improved theranostics [152]. PS-NPs have also been applied for MRI applications. In a simpler approach, a PS-MRI contrast agent Gd(III)-meso-tetrakis(4-pyridyl) porphyrin has been conjugated with chitosan NPs by passive adsorption, and investigated for its MRI contrast agent property [153]. While more complex nanoformulation designing involved multifunctional NPs of DOX@PLA@Au-PEG-MnP, which was fabricated of gold nanoshell surrounding doxorubicin (DOX) entrapped poly (lactic acid) core. Mn-porphyrin derivatives were coated on the surface of the gold shell through PEG linkage. Herein the gold nanoshell acted as NIR photon absorber, DOX as chemotoxic drug and Mn-porphyrin for PDT and MRI. These NPs exhibited synergistic chemo and photo-therapeutic effect and facilitated the imaging of locations and detailed structure of the tumor in nude mice through MRI [39,154].

Another strategy for designing nano PS-MRI contrast agents involve paramagnetic-porphyrins coated on magnetic particles core. Huang et al. strategically designed multifunctional PS based theranostic NPs where Ce6 was covalently linked on the surface of magnetic NPs (MNPs). Further during the investigation, Ce6-MNPs were observed to preferentially target tumors by application of external magnetic fields in gastric cancer mice model. Thus, this study demonstrated the successful design of targeted multifunctional magnetically guided PS delivery formulation as potential candidates with *in vivo* dual-mode NIR/FLI and MRI-guided PDT [155]. Similarly, HSA coated MNPs loaded with bacteriochlorin, porphyrin linked silica-coated MNPs, TPPS4 coated water-soluble Fe₃O₄ MNPs, self-assembled polymeric nanocapsules with dendrimer porphyrin incorporated in SPIONS, dextran-coated MNPs bearing porphyrin, ZnPC encapsulated silica-coated MNPs based porous microspheres and many other such nano-formulations have been evaluated for MRI-guided PDT [36,39,156,157]. MacDonald et al., reported the development of an organic, photonic NP, Mn(II)-porphyrin (porphyrin-lipid) as potent MRI-photothermal NP, also capable of PTT and PA tomography [78].

Contrary to inorganic NPs, theranostic protein NPs have also been explored for cancer imaging and therapy, but with a very limited successful outcome.

Few protein-based NPs utilizing viral capsid protein structure and other human proteins have been explored with PS for MRI and PDT applications. Paramagnetic Mn(III) Pp IX complexed with bacteriophage P22 capsid template and cowpea chlorotic mottle virus (CCMV) protein cage NP incorporated with Gd(III)-DOTA ligands and ZnPC have been explored as MRI contrast agents along with their potent PDT efficacy [158,159]. While in another work, Zhou et al., investigated size-tunable Gd₂O₃@albumin conjugating Ce6 (GA-NPs) using hollow albumin as the nanoreactor for MRI-guided photo-induced therapy [160].

Overall, MRI is considered to be one of the significant molecular imaging modalities owing to its excellent temporal and spatial resolution of micrometers with non-invasive methodology, unlimited tissue penetration, non-exposure to ionizing radiation, high soft tissue contrasts together with 3D, real-time imaging. However, MRI suffers from poor sensitivity, high cost, slow image acquisition, long post-processing times and administration of higher concentration of contrast agents [161]. Moreover, various factors need to be considered for application of metalloporphyrin-based conjugates and NP materials as a potential contrast agent for MRI. Rationale designing of PS-MRI contrast agents with enhanced relaxivities, increased contrast effect and brightness, stability against demetallation under physiological conditions and target specific biodistribution is highly desirable research area.

Positron Emission Tomography/ Single Photon Emission Computed Tomography Imaging combined Photodynamic Therapy

PET/SPECT, radiotracer-based noninvasive imaging techniques have gained extensive interest in the field of cancer diagnostics. PET imaging which is based on the radioactive decay of positron-emitting isotopes, provides functional, metabolic and molecular assessment of normal and diseased tissues [146]. PET radiotracers emit a positron (a positively charged electron) which in turn interacts with a surrounding free electron causing an annihilation reaction. This annihilation reaction results in the simultaneous production of two 511-KeV gamma rays (photons) at ~180° to each other which are further detected by the PET camera to generate an image. PET with 2-deoxy-2-[fluorine-18]-fluoro-D-glucose (¹⁸F-FDG), an analog of glucose, is the only PET probe approved by the Food and Drug Administration (FDA) for diagnosing, staging, restaging and detecting recurrence and treatment outcomes of various cancers to guide patient care in clinics. ¹⁸F-FDG, provides valuable functional information

based on the increased glucose uptake and glycolysis of cancer cells and depicts metabolic abnormalities [162]. ^{18}F -FDG-PET allows planning, therapeutic response monitoring to PDT along with real-time monitoring of PDT mediated systemic transient metabolic changes in cells (apoptosis, necrosis, proliferation, metabolism) and vascular damage [163,164]. Although ^{18}F -FDG is an effective tumor-localizing tracer, it is not tumor-specific. Moreover, the short half-life of ^{18}F -isotope (110 min) limits its use in PDT studies, due to considerably longer time of PSs to both accumulate in tumors as well as eliminate from the non-targeted organs [146]. Thus, this necessitates the use of radiolabeled PS to evaluate the PS biodistribution itself. Similar to the simple chemistry of formation of metallo-PS complexes, PS can be radiolabeled via simple complexation chemistry, due to their metal chelation property [165]. Radiolabeling of tetrapyrroles with Cu-64 for the localization of brain tumors and to develop coincident scintillation counters was first reported in 1951. Still, thereafter due to the technical limitations of earlier PET scanners, efforts to investigate the utility of ^{64}Cu -labeled PSs as PET probe were very disappointing. It was only in the 1980s, when Wilson et al., attempted to detect brain tumors using ^{64}Cu -Hp for *in vivo* measurements of its tumor uptake through PET imaging. However, the results of this study failed to gain interest, due to the poor tumor localization ability of ^{64}Cu -Hp and the poor spatial resolution of PET scanners at that time. Nevertheless, this study provided a valuable result that ^{64}Cu -labeling did not alter the main characteristics (biodistribution, pharmacokinetics, clearance) of the host PS molecules [166–168].

Among all the available PET radioisotopes, ^{64}Cu labeled tetrapyrrole PSs especially porphyrins have been extensively studied as promising PET probes, because of the ability of tetrapyrroles as ^{64}Cu chelator. Furthermore, photophysical properties and tumor-specific uptake of the macrocyclic PSs, long half-life of the Cu-64 isotope together with their biological compatibility, thermodynamic and kinetic stability made ^{64}Cu -PS complexes an attractive option not only for PET as well as for therapeutic applications [169].

A ^{64}Cu labeled metal-free sulfonated metallophthalocyanines ^{64}Cu -CuPcS was evaluated for biodistribution studies in tumor-bearing rats using small animal-PET. However, the results showed most of the ^{64}Cu activity within the kidneys and liver, with low uptake in tumor [170]. Similar effects were found in studies with other Cu-64 labeled PSs such as ^{64}Cu -5,10,15,20-tetrakis(penta fluoro phenyl) porphyrin, ^{64}Cu -labeled tri and tetra sulphonated

phthalocyanines [171,172]. Rong et al., developed HPPH loaded PEG-functionalized graphene oxide (GO), forming GO-PEG-HPPH complex. Following radiolabeling of HPPH with ^{64}Cu , *in vivo* biodistribution and delivery were tracked by PET, revealing increased tumor uptake of the complex resulting in improved photodynamic cancer cell killing efficacy [173]. Shi et al., demonstrated a ^{64}Cu labeled pyropheophorbide- α -peptide (GDEVDG SGK)-folate (^{64}Cu -PPF) as a targeted PET imaging probe for folate receptor (FR)-positive tumors along with fluorescent/PDT property. Selective uptake of ^{64}Cu -PPF in FR positive tumors was evident from high tumor-to-muscle ratio of 8.9, observed 24 h post-injection in a nude mice tumor model. Further, half-life of Cu-64 (12.7 h) was found to be compatible with the pharmacokinetics of PPF, thus providing adequate time for accumulation of ^{64}Cu -PPF at tumor sites followed by PET imaging [168]. Moreover, this concept was advanced to NPs, by direct inclusion of a radionuclide (Cu-64) into preformed organic, nontoxic, biodegradable porphyrins (porphyrin-lipid conjugates) forming ^{64}Cu -porphyrins. As only a fraction of the porphyrin is directly labeled with ^{64}Cu , this preserves NIR fluorescence property of porphyrins. *In vivo* bimodal (PET/FL) imaging of ^{64}Cu -porphyrins in tumor mice model, showed that ^{64}Cu -porphyrins can clearly delineate tumor tissues [174,175]. Further, Zheng et al., validated the *in vivo* sensitivity and selectivity of ^{64}Cu -porphyrins in clinically relevant orthotopic prostate and bony metastatic cancer models by dual-mode PET/FLI. The study demonstrated ^{64}Cu -porphyrins clearly delineated hypoxic orthotopic tumors on both the macro- and the microscopic scales and detected small bony metastases with high sensitivity [174]. Later, the same group reported another strategy, where porphyrin (pyropheophorbide)-phospholipid (PoP)-coated UCNP was utilized for seamless post labelling with ^{64}Cu for PET imaging. This ^{64}Cu labeled PoP-UCNP demonstrated *in vivo* lymphatics imaging using 6 different imaging modalities via FLI, UCLI, PET, CT, Cerenkov luminescence, and PA tomography [20]. The concept of seamless ^{64}Cu labeling of porphyrins was expanded by developing a soluble Meso-tetra(4-carboxyphenyl) porphyrin (mTCPP)-PEG polymeric mesh as whole-body PET or multimodal imaging probe for renal function monitoring. PET and FLI imaging showed rapid clearance of mTCPP-PEG via renal excretion in healthy mice but not in mice with acute renal failure [176]. Similarly, another surfactant-stripped micelle of pheophytin-a, was developed as a multimodal imaging agent. These Pheo ss-InFroMs were then seamlessly labeled with ^{64}Cu for whole body gut

imaging along with FLI and PAI [177].

Li et al., reported a robust, smart and highly versatile “all-in-one” porphyrin (pyropheophorbide)/cholic acid nanoconstruct (nanoporphyrin) which integrated several imaging (NIR FLI, PET, MRI), and therapeutic (PTT, PDT) functions in a single entity. These nanoporphyrins were seamlessly labeled with ^{64}Cu . PET imaging in ovarian cancer xenograft mice model revealed highest accumulation of nanoporphyrins in tumors at 24 h post injections with low background in the rest of the body. Further to gain accurate diagnosis this approach was extended by developing a dual-modality PET-MRI nanoprobe by incorporating both $^{64}\text{Cu}(\text{II})$ and $\text{Gd}(\text{III})$ into nanoporphyrins. Interestingly, combined MRI-PET imaging indicated inhomogeneous uptake and distribution of nanoporphyrins in the tumor [178]. Feng et al., prepared a multipurpose liposome by encapsulating hydrophilic banoxantrone (AQ4N) into its aqueous cavity and hydrophobic hexadecylamine conjugated Ce6 in the hydrophobic bilayer, forming AQ4N-hCe6-liposome. These liposomes demonstrated improved therapeutic outcomes in tumor-bearing mice via sequential PDT and hypoxia-activated chemotherapy. Chelation of ^{64}Cu with Ce6 formed PET probe AQ4N- ^{64}Cu -hCe6-liposome allowing an effective PET imaging together with FLI and PAI which indicated selective accumulation of liposomes in tumors [83].

Although ^{64}Cu isotope has been extensively used for the synthesis of promising tumor-avid PS-based PET imaging agents. However, other isotopes have also been explored for the same. PSs have also been used for most common clinical PET radioisotope F-18 labeling. Li and colleagues used BF₂ unit of BODIPY dyes as ^{18}F - radiofluorination site. They utilized the ^{18}F -PET/FL imaging modalities to study the biodistribution of the complex in *in vivo* tumor model which showed its maximum accumulation in the liver and kidneys [179]. However, the short half-life of ^{18}F limits its utilization for PS labeling and thus, alternatively, I-124 offers to a better candidate for PS labeling due to its long half-life of 4.2 days. MicroPET imaging revealed selective accumulation of Iodo-PK 11195 conjugated 3-[10-hexyloxyethyl]-3-devinyl pyropheophorbide-a HPPH in Translocator protein (TSPO) expressing tumor in mice model showing improved *in vivo* PDT efficacy [180]. Pandey and colleagues also reported other ^{124}I labeled purpurinimide and ^{124}I - labeled Methyl Pyropheophorbide-a [146,181]. Other than I-124, ^{62}Zn (half-life 9.26 h) labeled glycoconjugated 5,10,15,20-tetrakis(pentafluorophenyl)porphyrin also proved its cancer-selective accumulation property through *in vivo* PET imaging, with tumor to normal tissue uptake

ratio of four [182].

Similar to PET, SPECT is another radionuclide-based imaging modality that uses gamma-emitting radioisotope tracers like Technetium-99m, Iodine-123, Iodine-131, Indium-111. Gamma-rays (photons) emitted from SPECT radiotracers are then detected by collimated radiation detectors to generate images. Although both PET and SPECT have their own advantages and disadvantages, as compared to SPECT, PET provides better contrast and spatial resolution. Few studies have been carried out on utilization of PSs for chelation and imaging of SPECT tracers. Some of the examples includes Rhenium-188 (^{188}Re)-ICG micelles, Gallium-67 (^{67}Ga)-tetra phenyl porphyrin, Indium-111 (^{111}In)- Meso tetrakis (4-hydroxyphenyl) porphyrin, Technetium-99m ($^{99\text{m}}\text{Tc}$)-porphyrins, which have shown promising results for SPECT imaging for biodistribution and tumor uptake studies in mice model [183–186]. Furthermore, in a clinical study, In-111-Photofrin-II was investigated for its uptake and distribution in 20 patients with intracranial neoplasms, using SPECT. The results showed variations in kinetics of complex uptake according to the tumor histology, the patient's use of steroids, and even among patients with similar types of tumor histology, which allowed personalized PDT planning [187].

Nuclear imaging modalities have the advantages of providing quantitative information at biochemical and molecular level with an excellent nanomolar to picomolar imaging sensitivity without deep tissue penetration limitations. However, as imaging modality, both PET and SPECT suffers from safety issue due to use of radionuclides, being costly with slow image acquisition times, and cannot be used for long-term studies due to radiolabel decay. Furthermore, clinicians always prefer to combine nuclear imaging with other complementary imaging techniques such as MRI and/or CT due to the lack of good spatial resolution and anatomical information in PET/SPECT imaging [161]. Designing of PS-radioisotope conjugates or NPs requires careful consideration of the type of radionuclide and radiolabeling strategy, high *in vivo* stability and potential long-term toxicity. Another importance of employing radiolabelled (β -emitters) PS conjugates or NPs, is in Cherenkov Radiation Energy Transfer for exciting PS deep in the tissue without the application of an external light source as self-exciting “auto-PDT” [188]. Radiolabeled PSs are useful for localizing the biodistribution of PS mainly in the tumor mass and for PS uptake studies; however, they cannot be used for visualization of post-PDT effects due to the loss of PS selectivity and uptake by tumor tissue.

Consequently, different non-specific radiotracers are of interest to monitor and predict post-PDT response earlier than morphological imaging techniques like MRI and CT. Some of which includes: glucose metabolism with ^{18}F -FDG for studying tumor vasculature damage and direct cell death; tumor proliferation with ^{18}F -fluorodeoxythymidine; apoptosis with ^{64}Cu -DOTA-biotin-Sav and $^{99\text{m}}\text{Tc}$ -AnnexinV; hypoxia with ^{123}I -iodoazomycin arabinoside and tumor vascular damage with $^{99\text{m}}\text{Tc}$ -hexakis-2-methoxyisobutyl isonitrile or $^{99\text{m}}\text{Tc}$ -hexamethylpropyleneamine oxime etc [164].

Ultrasound Imaging combined Photodynamic Therapy

US imaging is one of the well-established, convenient and economical imaging techniques among all standard imaging modalities, due to its non-invasive real-time imaging nature, safety, non-usage of ionizing radiation, broad diagnostic applicability and easy handling. US imaging makes use of sound waves to produce an image of the tissue, based upon the differential interaction of sound waves with living tissue to provide quantitative structural and functional information of target organ and the velocity of moving tissue, primarily blood flow which can be easily visualized by US Doppler-effect mode. Furthermore, it is an established clinical imaging technique for identifying tumors and assessing disease progression via monitoring changes in tumor volume, lesion boundaries as cancer tissues have different echogenicity in comparison to healthy surrounding tissues. Thus, US imaging allows monitoring of structural, morphological and vasculature changes of tumor post-PDT and also provides information on apoptotic cell death [11,189].

Although conventional US imaging has better sensitivity to distinguish between normal and malignant tissues, its specificity is weak. In this regard, the use of US contrast agents provides improved sensitivity and high resolution of US imaging. Conventional US contrast agents are fluorinated gas-filled MBs stabilized by an outer shell of proteins, lipids, and polymers which are actively being used for Contrast Enhanced Ultrasound Imaging (CEUS). Cornelis et al., demonstrated the use of lyophilized MBs for CEUS imaging of tumor necrosis following WST11 (Tookad)-based PDT-inducing Vascular Targeted Photodynamic Therapy (VTP) in tumoral mice model. Although this study does not involve investigation of tumor growth kinetics or survival benefits based on CEUS of VTP of tumors, while the CEUS images showed good correlation with histology images of necrotic regions in tumors [190]. Additionally, certain preclinical

studies have investigated the use of MBs for molecular imaging, US-triggered drug and gene delivery. In this regard, Huynh et al., make use of MBs as PS delivery agents, wherein the “porphe microbubbles”, formed from a porphyrin-lipid shell encapsulating a fluorinated gas, for their *in vivo* US imaging of tumor mass in mice xenograft model [79,80]. However, these MBs have a short half-life in circulation as they are easily destroyed by diffusing away from the gas at body temperature. Moreover, owing to their micron size, these MBs are not able to extravasate and accumulate in tumor mass or penetrate the deep tissue layers. Thus, this necessitates the need for developing effective US contrast agents with a long half-life, enhanced stability and tumor selectivity for tumor tissues diagnostics [191].

Huynh et al., advanced the concept of porphe MBs to low-frequency US induced conversion of MBs to NPs. They synthesized perfluoropropane gas encapsulated bacteriochlorophyll-lipid shell MBs for trimodality contrast agents for US, PA and FL imaging, where the encapsulated gas provides US imaging contrast and the bacteriochlorophyll PS in the shell confers PA and fluorescent properties. Upon exposure to US, the MBs (1-10 μm) disintegrates and forms smaller NPs (5-500 nm) that retain the encapsulated payload of PSs and possesses the same optical properties as the original MBs. They further validated this concept in xenograft tumor-bearing mice model and suggested their PDT application [192]. Later on, You et al., exploited the concept of US conversion of MBs to NPs and demonstrated that porphyrin-grafted lipid (PGL)-MB allowed favourable CEUS imaging outcome. Transformation of PGL-MBs into PGL-NPs upon US exposure, demonstrated exceptional accumulation ability at the tumor site via sonoporation effect. Thus, PS loaded MBs act as a good candidate for assisting targeted PDT in cancer theranostics, due to their enhanced US contrast to better localize tumor lesions, and targeted delivery of PS by virtue of ultrasound targeted microbubble destruction (UTMD) [193]. The importance of nanobubbles (NBs) in CEUS imaging was further investigated by Huang and colleagues where they investigated NBs encapsulated mesoporous silica-coated gold nanorod UCNP along with merocyanine 540 as PS (MC540-AuNR@UCNP@NB). This hybrid nanosystem allowed enhanced US imaging along with AuNR@UCNP mediated excitation of merocyanine 540 to improve NIR PDT [94]. Park et al., reported Ce6-loaded pH-responsive bubble-generating CaCO_3 -mineralized NPs (Ce6-BMNs) having the potential for US imaging-guided PDT of tumors. Ce6-BMNs exhibited significant stability

under physiological conditions and effectively inhibited Ce6 release at physiological pH (7.4). At tumoral acidic pH (6.4), dissolution of the CaCO_3 mineral core allows CO_2 bubble generation which resonates under applied US field and simultaneously triggers the release of Ce6 due to UTMD. This allows for greatly enhanced US signal-guided PDT for cancer theranostics [191]. Figure 8 represents the schematic principle for the application of MBs mediated US-assisted imaging and guided PDT.

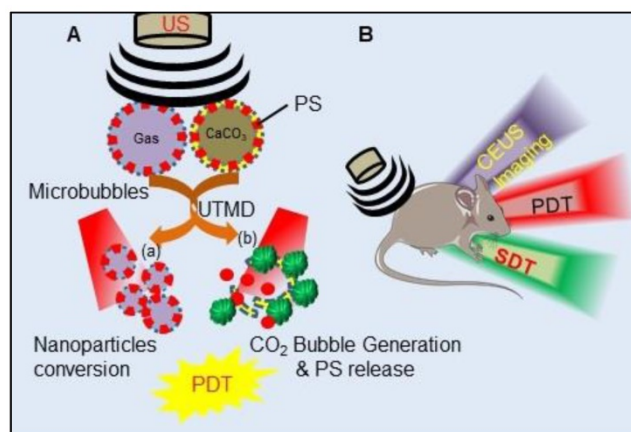


Figure 8. Schematic illustration of microbubble mediated ultrasound-assisted imaging and guided Photodynamic Therapy (PDT): A. Ultrasound (US) targeted microbubble destruction (UTMD) followed by (a) induced transformation of microbubbles to nanoparticles, (b) CO_2 generation and photosensitizer (PS) release, resulting in tumoral uptake and *in vivo* PDT; B. Illustration of US induced Contrast Enhanced Ultrasound (CEUS) imaging, PDT and Sonodynamic Therapy (SDT).

Similarly, some other PS-embedded CaCO_3 NPs have been investigated for US imaging-guided PDT [194,195]. Huang and colleagues reported the synthesis of dendritic mesoporous organosilica NPs encapsulating ICG and catalase (ICG-CAT@MONs) to overcome the tumor hypoxia induced PDT limitation and PA/US-guided tumor ablation. Upon light excitation, encapsulated ICG results in simultaneous PAI and PDT of *in vivo* tumor tissues, while the catalase molecules catalyze the decomposition of endogenous H_2O_2 into O_2 bubbles to intensify US imaging signal and enhance PDT efficacy simultaneously. Thus, the results showed excitation of ICG-CAT@MONs causes enhanced tumor destruction due to the sustainable O_2 generation, eventually promoting PDT and holds promise in multimodal PA/US image-guided PDT [196]. In another exciting discovery, Sun and collaborators reported the synthesis of multifunctional PGL MBs loaded with HIF-1 α siRNA (siHIF@CpMB) for PDT combined with gene therapy in triple-negative breast cancer therapy. US imaging allowed real-time monitoring of siHIF@CpMB distribution. Furthermore, UTMD of siHIF@CpMB efficiently converts them into NPs promoting the accumulation of porphyrin and siRNA

at the tumor site via the cavitation effect. HIF-1 α siRNA downregulates HIF1 α expression in the hypoxic tumor region, ultimately relieving hypoxia-induced ROS generation during PDT and thus improves the overall therapeutic outcome. In a similar study, PGL MBs were shown to achieve US-controlled PS accumulation in tumors and enhanced US-assisted PDT efficacy in *in vivo* prostate cancer mice model [197].

Presently, the US technique is widely applied for imaging and diagnostics in clinical setups, owing to its safety, non-invasiveness, good tissue penetration ability, low operation, and instrumental costs. Further, targeted PS based CEUS is an emerging imaging strategy for evaluating biological processes at the molecular level, also known as the molecular US imaging, which is based on sophisticated PS - US contrast agent designing as discussed in this section. However, US imaging suffers from low resolution, and usually fails to accurately determine lesion size, boundaries, and fine details of the anatomy of deep tissue which leads to operator variability. Further technical advancements like the introduction of better light delivery systems, US transducers with better sensitivity, faster data acquisition, advanced computed 3D reconstruction and better image processing algorithms can overcome the inherent limitations and will establish the utility of US imaging in PDT dosimetry and treatment monitoring [11]. Many commonly used PSs such as Hp, ALA, Ce6, Pheophorbide a, ZnPc etc., have shown to act as sonosensitizers. Activation of sonosensitizers by US exerts anticancer therapeutic effects through sonodynamic therapy (SDT) by generating ROS. Consequently, the combination of PDT and SDT delivers improved therapeutic effects from surface to the significant tissue depth, due to deep tissue targeting by focused US energy compared to visible light penetration [198].

X-ray Computed Tomography combined Photodynamic Therapy

CT imaging is an age-old computerized X-ray based, cost-effective imaging modality in clinics that uses the combination of a narrow beam of X-rays to generate cross-sectional images or "slices" of the body, known as tomographic images. Numerous successive slices are then digitally "stacked" together to form a 3D image of the body or body organs that allows localizing possible tumors. As compared to conventional X-ray images, CT generates a cross-sectional image with 3D anatomic details for both soft and hard tissues. In clinics, X-ray attenuating contrast media containing heavy elements (most commonly Iodine or Barium) are used to generate CT

images of soft tissues with high contrast to the surrounding tissues [199,200]. In this regard many heavy atoms based nanoformulations have been utilized for CT imaging combined PDT. For example, Yin and colleagues utilized gold as an X-ray attenuation element to develop a meso-tetrakis(4-carboxyl)-21H,23H-porphine (TCPP) covalent organic polymer (COP-8) and β -cyclodextrin (β -CD) functional AuNPs, COP@Au@TCPP nanocomposites for gold-based CT-image-guided PDT. Moreover, decomposition of H_2O_2 into O_2 catalyzed by CD-AuNPs in tumor cells further assisted in overcoming the limitation of hypoxia-induced PDT efficacy of TCPP [200]. In another study, a biocompatible PEGylated nanoliposomes co-encapsulating clinically approved Iodinated CTIA iodixanol (Visipaque®) and a PS TPPS4 demonstrated enhanced PDT guided by CT imaging [201]. Similarly, many other nanoformulations combining heavy element and PS have been reported as a promising agent for CT imaging combined with PDT [86,202–208].

X-ray CT is one of the most extensively used cost-effective clinical imaging techniques which allow deep tissue and/or whole-body imaging with high spatial resolution and 3D visualization with fast image acquisition and processing time. However, as compared to MRI, CT suffers from safety issues due to the use of high-energy ionizing radiations and also less efficient in contrasting soft tissues. Combination of CT with other imaging techniques like highly sensitive OI and molecular imaging like MRI and nuclear imaging techniques can exhibit great advantages in cancer theranostics. However, studies of CT using PS-based CT contrast agents have been restricted to *in vivo* small animals using microCT. Therefore, improvement in detectors and spatiotemporal CT scanners hold promise for deployment of CT in clinics as multimodal imaging advancements.

Tumor Microenvironment Responsive Activatable Photosensitizers: For Selective Photo-Theranostics

Although image-guided laser irradiation and targeted PS provides preferential tumor targeting, they still cannot completely overcome the side effects of non-targeted tissue photodamage. Therefore, an advanced strategy for developing aPS with higher selectivity and efficiencies as smart phototheranostic agents has gained current research interest [4,27]. As compared to traditional PSs, activatable photothera-

nostic PSs are strategically designed to respond to cancer-specific environmental stimuli which allow both molecular imaging and phototoxic effects at the target tumor site. More importantly, even after light exposure, aPS remains passive or unexcited in the absence of tumor-associated stimuli. This strategy allows higher tumor-selective accumulation and efficacy with minimal cytotoxicity to surrounding healthy cells and further offers higher imaging sensitivity as tumor molecular diagnostics demarcates target cancerous tissues from healthy tissues [33]. Designing and developing efficient aPSs needs to take into consideration (i) introducing proper stimuli-responsive linkers or groups; (ii) properties like high PS activation efficiency including both 1O_2 quenching in its deactivated state and reactivation; to impart high therapeutic efficacy of PDT with minimum side effects. Various natural and biodegradable polymers e.g. polylactide (PLA), poly(ϵ -caprolactone) (PCL), poly(lactic-co-glycolic acid) (PLGA), pluronic, polyphosphoester, hyaluronic acid (HA), dextran, and chondroitin sulfate have been utilized as stimuli-responsive polymeric nanovehicles for delivery of various PSs. PSs are usually introduced into these polymeric nanoformulations either by chemical conjugation with the polymers or physically being encapsulated into nanosystems [67,209]. Advantages of stimuli-responsive nanoformulation involve higher stability and reduced premature activation of PS, due to its self-quenching effect, which all together minimizes the side effects while in circulation and only are activated in targeted sites to induce effective PDT outcomes. Designing strategies of various novel stimuli-responsive PS based nanocarriers in response to various intracellular and tumor microenvironment-based stimuli such as pH, antioxidants, specific enzymes, ATP, ROS, redox-potential and hypoxia have already been reviewed [4,6,27,33,34,210–212]. The following section presents some representative tumor microenvironment-responsive aPSs inducing targeted phototoxicity combined with various imaging modalities (Table 4).

In comparison with conventional “always-on” PSs, tumor microenvironment responsive “turn-on” PS nanoformulations offer the advantages of improving the sensitivity and resolution of imaging modalities. aPSs usually amplify imaging signals at the target site together with reducing the background signals and/or autofluorescence (for FLI), which consequently increases the SNR and reduces the limit of detection.

Table 4. Representative theranostic activatable photosensitizers as conjugates and nanoparticles for simultaneous imaging and Photodynamic Therapy.

Activating factor	PS and Nanoformulation	Targeting moiety	Imaging technique	Reference
Low pH	aza-BODIPY (NEt ₂ Br ₂ BDP) Cyclic arginine-glycine-aspartate motif (cRGD)-functionalized nanomicelle	cRGD for αvβ3 integrin-rich tumor cells.	NIR	[213]
	Chlorin e6 (CaCO ₃ -mineralized NPs)	--	US	[191]
	Methylene Blue (CaCO ₃ nanorods)	--	US	[195]
	Pheophorbide-a (FA-BSA-c-PheoA)	Folate	NIR	[214]
	Zn(II) phthalocyanine (Layered double hydroxide-PcS supramolecular nanohybrid)	--	FLI	[215]
Hyaluronidase	Sinoporphyrin sodium (Manganese-doped calcium phosphate mineralized glucose oxidase nanoparticles)	--	FLI and MRI	[65]
	Indocyanine green (Mesoporous silica-coated gold nanorods)	--	FLI and PAI	[216]
	Indocyanine green (MnO ₂ modified hyaluronic acid NPs)	Hyaluronic acid for CD44 receptor binding	FL and PAI	[217]
Reducing TME	Chlorin e6 (HA-ADH-Ce6 NPs)	Hyaluronic acid for CD44 receptor binding	NIR and PAI	[218]
	Chlorin e6 (Ce6-heparin- alpha-tocopherol succinate)	--	NIR	[219]
	Chlorin e6 (Ce6- dextran conjugates nanoformulations)	--	NIR	[220]
	Chlorin e6 (Ce6-fucoidan conjugates nanogels)	Fucoidan for P-selectin surface protein	NIR	[221]
Low pH & reducing TME	Chlorin e6 (α-cyclodextrin (α-CD) and poly (ethylene glycol) -Ce6)	--	NIR	[222]
	Toluidine blue (FeOOH modified NaLuF ₄ :Yb,Er,Tm@NaLuF ₄)	--	UCL	[95]
	Chlorin e6 (CNT@MnO ₂ -PEG@Ce6 carbon nano tubes)	Folate terminated aminated poly (ethylene glycol) (FA-PEG-NH ₂)	MRI	[223]
H ₂ O ₂	Pro-photosensitizer (MBPB) converted to active methylene blue (BSA-MBPB nanoformulations)	--	NIR and PAI	[224]
Low pH and H ₂ O ₂	Chlorin e6 (Ce6/MnOx@HMSNs-PEG)	--	MRI	[225]
	Methylene blue (SiO ₂ -MB@MnO ₂)	--	MRI	[226]
Reducing TME and matrix metalloproteinase	Chlorin e6 (PEGylated Ce6-MMP2 NPs)	Matrix metalloproteinase 2	NIR	[227]
Biomolecules responsive				
Albumin	Zn(II) phthalocyanine (Self-assembled supramolecular nanovesicle)	--	FLI	[228]
Nucleic acid	Zn(II) phthalocyanine (Mitoxantrone and Zn(II) phthalocyanine supramolecular nanoassembly)	--	FLI	[229]
Biotin	Zn(II) phthalocyanine (Phthalocyanine - triethylene glycol self-assembled nanoformulations)	Biotin moiety	FLI and PAI	[230]

NIR: Near Infrared Imaging; MRI: Magnetic Resonance Imaging; PAI: Photoacoustic Imaging; UCL: Upconversion Luminescence Imaging; US: Ultrasound Imaging; FLI: Fluorescence Imaging; NPs: Nanoparticles; TME: Tumor microenvironment

Conclusions and Future perspective

Since the first approval of PDT in 1995 as an esophageal cancer treatment modality, due to its feasibility and effectiveness, it has made conspicuous progress clinically to establish itself as a treatment strategy for other cancers as well. Although PDT has proved its tremendous potential for being an efficacious treatment strategy against cancer, its application is still restricted as an adjunct therapy and palliative care for cancer patients [11]. One of the main setbacks in PDT or other cancer therapies involve lack of proper dosimetric strategies in evaluating actual drug dose at the tumor site for envisaging therapeutic response and planning of subsequent therapies. Molecular imaging modalities like conventional OI, MRI, PET, US and CT are able to provide detailed structural, functional and molecular information about pre- and post-therapeutic conditions of the tumor. However, they cannot provide real-time monitoring because of the use of different agents for imaging and therapy. In this regard due to its favorable and fascinating chemistry, PSs can be easily modified into theranostic agents for

application in almost all available imaging techniques or multimodality imaging combined with PDT [231,232]. In this review, we have discussed molecular design rationales for PSs that have been pursued for the development of multifunctional theranostic agents. Nanotechnology has further widened the scope of this research area as it allows to explore “two-in-one” or “multiple-in-one” imaging parameters in a single nanoformulation along with tumor-targeting properties. Application of smart aPS summarized in this review can simultaneously activate their imaging signals and phototoxic effects in response to cancer-specific stimuli such as pH, ROS, cancer-associated enzymes, proteins etc. Compared to always-on theranostic agents these aPSs have the advantages of (a) higher diagnostic specificity and sensitivity, (b) improved and selective treatment efficacy, and (c) minimum systematic side-effects.

Although the research of developing PS-based theranostic agents with multimodal imaging abilities has recently gained momentum, they are still under the growth stage. Despite the progress in strategic designing of novel PS-based theranostic agents,

currently available non-activatable and activatable formulations are majorly based on the inherent FLI-guided PDT. Although other imaging techniques offer more effective and accurate diagnostic information, due to the limited choice of materials/metals, they have been less explored. As the designing and development of such multifunctional agents are mainly based on nanomaterial formulations and nonbiological elements, few serious issues need to be addressed before pushing such agents into clinical trials. Dose, pharmacokinetics and potential toxicity of such formulations need to be further investigated for the purpose of clinical translation. Further, the *in vivo* metabolism of nanomaterials should be studied in detail as their clearance pathway is through the reticuloendothelial system. Especially non-degradable nanomaterials require weeks for clearance from the body and accumulates in high concentration in the reticuloendothelial organs increasing the risk of damage to the human body and organs. Hence, clearance optimization of such nanomaterial-based agents needs to be designed in such a manner as to reduce their dimensions (~5 nm) by enhancing their *in vivo* biodegradability for renal clearance [33,233]. Other than strategic designing, and *in vivo* toxicity and effectiveness assessment of phototheranostic agents, several technical obstacles need to be addressed for each imaging modalities. As already discussed, all the imaging techniques suffer from their intrinsic limitations, however, technical advancement

at the image acquisition and processing level such as improvement in sensitivity of detectors and equipments, image processing and 3D reconstruction algorithms and faster data acquisition can assure better imaging outcomes for effective PDT.

In summary, as represented in Figure 9, PS based multifunctional theranostic agents hold great potential to make personalized and integrated therapy feasible. Further, integrating different clinically available MRI, CT, PET, US with more advanced imaging modalities like optical, PA, SERS increases imaging penetration depth, diagnosis accuracy, and sensitivity for efficacious image-guided PDT to envision the era of personalized medicine.

Abbreviations

$^1\text{O}_2$: Single Oxygen; AIE: Aggregation Induced Emission; 5-ALA: 5-aminolevulinic acid; AIPcS4: Aluminum phthalocyanine tetrasulfonic Acid; aPS: Activatable photosensitizer; AgNPs: Silver Nanoparticles; AuNPs: Gold nanoparticles; BHQ: Black Hole Quenchers; Ce6: Chlorin e6; CEUS: Contrast Enhanced Ultrasound Imaging; CT: Computed Tomography; EPR: Enhanced Permeation and Retention; FA: Folic Acid; FDG: Fluorodeoxyglucose; FGS: Fluorescence-guided surgery; FL: Fluorescence; FLI: Fluorescence Imaging; GSH: Reduced Glutathione; GdDTPA: Gadolinium-diethylenetriaminepentacetate; Gd-DTTA: Gadolinium-(siloxyl-propyl)diethylenetriamine tetraacetate; GdDOTA: Gadolinium-tetraazacyclododecane tetraacetic acid; ICG: Indocyanine green; ISC: Intersystem crossing; HA: Hyaluronic acid; Hp: Hematoporphyrin; HPPH: 3-devinyl-3-(1-hexyloxyethyl) pyropheophorbide-a; H_2O_2 : Hydrogen peroxide; HSA: Human Serum Albumin; MB: Methylene blue; MBs: Microbubbles; MNPs: Magnetic Nanoparticles; MR: Magnetic Resonance; MRI: Magnetic Resonance Imaging; NBs: Nanobubbles; NIR: Near Infrared Radiation; NP: Nanoparticle; OCT: Optical Coherence Tomography; OI: Optical Imaging; PA: Photoacoustic; PAI: Photoacoustic imaging; PcS4: phthalocyanine tetrasulfonic acid; PDD: Photodynamic Diagnosis; PDT: Photodynamic therapy; PEG: Polyethylene Glycol; PGL: porphyrin-grafted lipid; PET: Positron Emission Tomography; PFD: Photosensitizer fluorescence detection; PpIX: Protoporphyrin IX; PS: Photosensitizers; PTT: Photothermal Therapy; RB: Rose Bengal; RIM: Restriction of intramolecular motions; ROS: Reactive Oxygen species; SERS: Surface-enhanced Raman scattering; SNR: Sound to Noise ratio; SPECT: Single-Photon Emission Computed Tomography; SPION: Superparamagnetic iron oxide nanoparticle; Sq: 2,4-bis[4-(N,N-dibenzyl-amino)-2,6-dihydroxyphenyl] squaraine; TB:

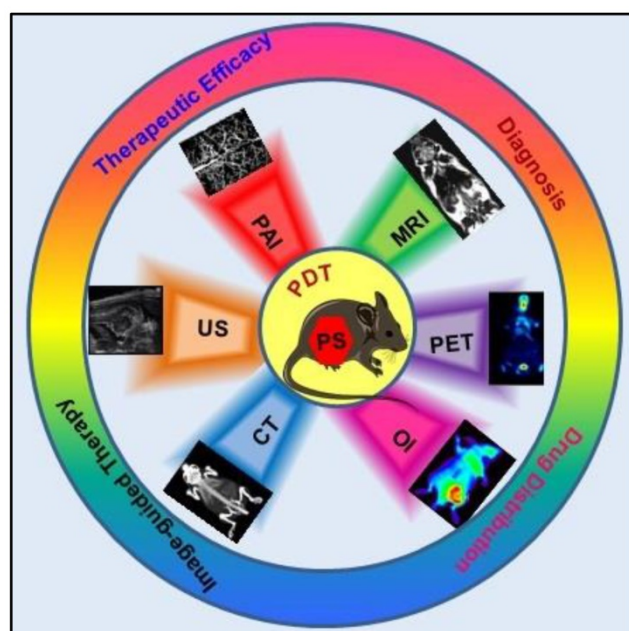


Figure 9. Theranostic Photosensitizers: Applications of theranostic photosensitizers (PS) in various imaging modalities: Magnetic Resonance Imaging (MRI), Positron Emission Tomography (PET), Optical Imaging (OI), X-ray computerized tomography (CT), Ultrasound Imaging (US), Photoacoustic Imaging (PAI).

Toluidine Blue; TPP: Tetraphenylporphyrin; TPPS4: Meso-tetra-(4-sulfonatophenyl) porphyrin; Tz: Tetrazine; UCL: Upconversion luminescence; UCLI: Upconversion luminescence Imaging; UCNP: Upconversion nanoparticle; US: Ultrasound; UTMD: Ultrasound targeted microbubble destruction; ZnPc: Zinc Phthalocyanine.

Acknowledgements

The authors sincerely thank the Department of science and technology and national Research foundation of South Africa and Laser Research Centre (LRC), University of Johannesburg.

Financial Support

This work is supported by the South African Research Chairs initiative of the Department of science and technology and National Research Foundation of South Africa (Grant No 98337), as well as grants received from the University Research Committee (URC), University of Johannesburg and the Council for Scientific and Industrial Research (CSIR)-National Laser Centre (NLC).

Competing Interests

The authors have declared that no competing interest exists.

References

- Sung H, Ferlay J, Siegel RL, Laversanne M, Soerjomataram I, Jemal A, et al. Global cancer statistics 2020: GLOBOCAN estimates of incidence and mortality worldwide for 36 cancers in 185 countries. *CA Cancer J Clin.* 2021; 0: 1-41.
- Lee LYW, Cazier JB, Starkey T, Briggs SEW, Arnold R, Bisht V, et al. COVID-19 prevalence and mortality in patients with cancer and the effect of primary tumour subtype and patient demographics: a prospective cohort study. *Lancet Oncol.* 2020; 21: 1309-16.
- Ethirajan M, Chen Y, Joshi P, Pandey RK. The role of porphyrin chemistry in tumor imaging and photodynamic therapy. *Chem Soc Rev.* 2011; 40: 340-62.
- Li X, Kolemen S, Yoon J, Akkaya EU. Activatable photosensitizers: agents for selective photodynamic therapy. *Adv Funct Mater.* 2017; 27: 1604053.
- Liu M, Li C. Recent advances in activatable organic photosensitizers for specific photodynamic therapy. *Chempluschem.* 2020; 85: 948-57.
- Yang M, Li X, Yoon J. Activatable supramolecular photosensitizers: Advanced design strategies. *Mater. Chem. Front.* 2021; 5: 1683-93.
- Kim MM, Darafsheh A. Light sources and dosimetry techniques for photodynamic therapy. *Photochem Photobiol.* 2020; 96: 280-294.
- Hu T, Wang Z, Shen W, Liang R, Yan D, Wei M. Recent advances in innovative strategies for enhanced cancer photodynamic therapy. *Theranostics.* 2021; 11: 3278-300.
- Li X, Lovell JF, Yoon J, Chen X. Clinical development and potential of photothermal and photodynamic therapies for cancer. *Nat Rev Clin Oncol.* 2020; 17: 657-74.
- Agostinis P, Berg K, Cengel KA, Foster TH, Girotti AW, Gollnick SO, et al. Photodynamic therapy of cancer: An update. *CA Cancer J Clin.* 2011; 61: 250-81.
- Hester SC, Kuriakose M, Nguyen CD, Mallidi S. Role of ultrasound and photoacoustic imaging in photodynamic therapy for cancer. *Photochem. Photobiol.* 2020; 96: 260-279.
- Deng X, Shao Z, Zhao Y. Solutions to the drawbacks of photothermal and photodynamic cancer therapy. *Adv Sci (Weinh).* 2021; 8: 2002504.
- Yang M, Yang T, Mao C. Enhancement of Photodynamic Cancer Therapy by Physical and Chemical Factors. *Angew Chem Int Ed Engl.* 2019; 58:14066-80.
- Fan W, Huang P, Chen X. Overcoming the Achilles' heel of photodynamic therapy. *Chem Soc Rev.* 2016; 45: 6488-519.
- Fass L. Imaging and cancer: A review. *Mol. Oncol.* 2008; 2: 115-52.
- Higgins LJ, Pomper MG. The evolution of imaging in cancer: current state and future challenges. *Semin Oncol.* 2011; 38: 3-15.
- Rieffel J, Chitgupi U, Lovell JF. Recent advances in higher-Order, multimodal, biomedical imaging Agents. *Small.* 2015; 11: 4445-61.
- Michalski MH, Chen X. Molecular imaging in cancer treatment. *Eur J Nucl Med Mol Imaging.* 2011; 38: 358-77.
- Kircher MF, Hricak H, Larson SM. Molecular imaging for personalized cancer care. *Mol Oncol.* 2012; 6: 182-95.
- Rieffel J, Chen F, Kim J, Chen G, Shao W, Shao S, et al. Hexamodal imaging with porphyrin-phospholipid-coated upconversion nanoparticles. *Adv Mater.* 2015; 27: 1785-90.
- Celli JP, Spring BQ, Rizvi I, Evans CL, Samkoe KS, Verma S, et al. Imaging and photodynamic therapy: mechanisms, monitoring, and optimization. *Chem Rev.* 2010; 110: 2795-838.
- Mallidi S, Spring BQ, Chang S, Vakoc B, Hasan T. Optical imaging, photodynamic therapy and optically triggered combination treatments. *Cancer J.* 2015; 21: 194-205.
- Abrahamse H, Hamblin MR. New photosensitizers for photodynamic therapy. *Biochem J.* 2016; 473: 347-64.
- Dąbrowski JM, Pucelik B, Regiel-Futyra A, Brindell M, Mazuryk O, Kyzioł A, et al. Engineering of relevant photodynamic processes through structural modifications of metallotetrapyrrolic photosensitizers. *Coord Chem Rev.* 2016; 325: 67-101.
- Zhang J, Jiang C, Figueiró Longo JP, Azevedo RB, Zhang H, Muehlmann LA. An updated overview on the development of new photosensitizers for anticancer photodynamic therapy. *Acta Pharm Sin B.* 2018; 8: 137-146.
- Zhao X, Liu J, Fan J, Chao H, Peng X. Recent progress in photosensitizers for overcoming the challenges of photodynamic therapy: from molecular design to application. *Chem Soc Rev.* 2021; 50: 4185-219.
- Lovell JF, Liu TWB, Chen J, Zheng G. Activatable photosensitizers for imaging and therapy. *Chem Rev.* 2010; 110: 2839-57.
- Li X, Lee S, Yoon J. Supramolecular photosensitizers rejuvenate photodynamic therapy. *Chem Soc Rev.* 2018; 47: 1174-88.
- Li X, Zheng BD, Peng XH, Li SZ, Ying JW, Zhao Y, et al. Phthalocyanines as medicinal photosensitizers: Developments in the last five years. *Coord Chem Rev.* 2019; 379: 147-160.
- Chen J, Fan T, Xie Z, Zeng Q, Xue P, Zheng T, et al. Advances in nanomaterials for photodynamic therapy applications: Status and challenges. *Biomaterials.* 2020; 237: 119827.
- Kelkar SS, Reineke TM. *Theranostics: combining imaging and therapy.* *Bioconjug Chem.* 2011; 22: 1879-903.
- Jenni S, Sour A. Molecular theranostic agents for photodynamic therapy (PDT) and magnetic resonance imaging (MRI). *Inorganics (Basel).* 2019; 7:10.
- Cheng P, Pu K. Activatable phototheranostic materials for imaging-guided cancer therapy. *ACS Appl Mater Interfaces.* 2020; 12: 5286-99.
- Zhang J, Ning L, Huang J, Zhang C, Pu K. Activatable molecular agents for cancer theranostics. *Chem Sci.* 2020; 11: 618-30.
- Yang ZS, Yao Y, Sedgwick AC, Li C, Xia Y, Wang Y, et al. Rational design of an 'all-in-one' phototheranostic. *Chem Sci.* 2020; 11: 8204-13.
- Calvete MJF, Pinto SMA, Pereira MM, Gerales CFGC. Metal coordinated pyrrole-based macrocycles as contrast agents for magnetic resonance imaging technologies: Synthesis and applications. *Coord Chem Rev.* 2017; 333: 82-107.
- Imran M, Ramzan M, Qureshi AK, Khan MA, Tariq M. Emerging applications of porphyrins and metalloporphyrins in biomedicine and diagnostic magnetic resonance imaging. *Biosensors (Basel).* 2018; 8: 95.
- Simões JCS, Sarpaki S, Papadimitroulas P, Therrien B, Loudos G. Conjugated photosensitizers for imaging and PDT in cancer research. *J Med Chem.* 2020; 63:14119-50.
- Shao S, Rajendiran V, Lovell JF. Metalloporphyrin nanoparticles: coordinating diverse theranostic functions. *Coord Chem Rev.* 2019; 379: 99-120.
- Tuchin VV. *Handbook of optical biomedical diagnostics.* 2nd ed. Vol 1. Washington, USA: SPIE; 2016.
- Wang C, Wang Z, Zhao T, Li Y, Huang G, Sumer BD, et al. Optical molecular imaging for tumor detection and image-guided surgery. *Biomaterials.* 2018; 157: 62-75.
- Xu X. Development and applications of optical imaging techniques in cancer diagnosis: diffuse optical tomography and microendoscopy. *Curr Med Imaging.* 2008; 4: 125-33.
- Balas C. Review of biomedical optical imaging—a powerful, non-invasive, non-ionizing technology for improving in vivo diagnosis. *Meas Sci Technol.* 2009; 20: 104020.
- Arranz A, Ripoll J. Advances in optical imaging for pharmacological studies. *Front Pharmacol.* 2015; 6: 189.
- Nguyen VN, Kumar A, Lee MH, Yoon J. Recent advances in biomedical applications of organic fluorescence materials with reduced singlet-triplet energy gaps. *Coord Chem Rev.* 2020; 425: 213545.
- Huang P, Lin J, Wang X, Wang Z, Zhang C, He M, et al. Light-triggered theranostics based on photosensitizer-conjugated carbon dots for simultaneous enhanced-fluorescence imaging and photodynamic therapy. *Adv Mater.* 2012; 24: 5104-10.
- He J, Yang L, Yi W, Fan W, Wen Y, Miao X, et al. Combination of fluorescence-guided surgery with photodynamic therapy for the treatment of cancer. *Mol Imaging.* 2017; 16: 1536012117722911.
- Iyer R, Wolf J, Zhukova D, Padanilam D, Nguyen KT. Nanomaterial based photo-triggered drug delivery strategies for cancer theranostics. In: Conde J

- Ed. Handbook of Nanomaterials for Cancer Theranostics. Elsevier; 2018: 351-91.
49. Eljamel MS, Goodman C, Moseley H. ALA and Photofrin fluorescence-guided resection and repetitive PDT in glioblastoma multiforme: a single centre Phase III randomised controlled trial. *Lasers Med Sci.* 2008; 23: 361-7.
 50. Stummer W, Pichlmeier U, Meinel T, Wiestler OD, Zanella F, Reulen HJ. Fluorescence-guided surgery with 5-aminolevulinic acid for resection of malignant glioma: a randomised controlled multicentre phase III trial. *Lancet Oncol.* 2006; 7: 392-401.
 51. Vermandel M, Dupont C, Lecomte F, Leroy HA, Tuleasca C, Mordon S, et al. Standardized intraoperative 5-ALA photodynamic therapy for newly diagnosed glioblastoma patients: a preliminary analysis of the INDYGO clinical trial. *J Neurooncol.* 2021; 152: 501-14.
 52. Zhang Y, Wan Y, Chen Y, Blum NT, Lin J, Huang P. Ultrasound-enhanced chemo-photodynamic combination therapy by using albumin "nanoglu" based nanotheranostics. *ACS Nano.* 2020; 14: 5560-69.
 53. Huang P, Lin J, Wang S, Zhou Z, Li Z, Wang Z, et al. Photosensitizer-conjugated silica-coated gold nanoclusters for fluorescence imaging-guided photodynamic therapy. *Biomaterials.* 2013; 34: 4643-54.
 54. Yan X, Niu G, Lin J, Jin AJ, Hu H, Tang Y, et al. Enhanced fluorescence imaging guided photodynamic therapy of sinoporphyrin sodium loaded graphene oxide. *Biomaterials.* 2015; 42: 94-102.
 55. Luby BM, Walsh CD, Zheng G. Advanced photosensitizer activation strategies for smarter photodynamic therapy beacons. *Angew Chem Int Ed Engl.* 2019; 58. doi: 2558-69.
 56. Mei J, Leung NLC, Kwok RTK, Lam JWY, Tang BZ. Aggregation-Induced Emission: together we shine, united we soar!. *Chem Rev.* 2015; 115: 11718-940.
 57. Hu F, Xu S, Liu B. Photosensitizers with Aggregation-Induced Emission: materials and biomedical applications. *Adv Mater.* 2018; 30: e1801350.
 58. Sansaloni-Pastor S, Bouilloux J, Lange N. The dark side: photosensitizer prodrugs. *Pharmaceuticals (Basel).* 2019; 12: 148.
 59. Moore AL, Joy A, Tom R, Gust D, Moore TA, Bensasson RV, et al. Photoprotection by carotenoids during photosynthesis: motional dependence of intramolecular energy transfer. *Science.* 1982; 216: 982-4.
 60. Reddi E, Segalla A, Jori G, Kerrigan PK, Liddell PA, Moore AL, et al. Carotenoporphyrins as selective photodiagnostic agents for tumours. *Br J Cancer.* 1994; 69: 40-5.
 61. Gurfinkel M, Thompson AB, Ralston W, Troy TL, Moore AL, Moore TA, et al. Pharmacokinetics of ICG and HPPH-car for the detection of normal and tumor tissue using fluorescence, near-infrared reflectance imaging: a case study. *Photochem Photobiol.* 2000; 72: 94-102.
 62. Tatman D, Liddell PA, Moore TA, Gust D, Moore AL. Carotenohematoporphyrins as tumor-imaging dyes. *Synthesis and in vitro photophysical characterization.* *Photochem Photobiol.* 1998; 68:459-66.
 63. Stefflova K, Chen J, Zheng G. Using molecular beacons for cancer imaging and treatment. *Front. Biosci.* 2007; 12: 4709-21.
 64. Chen J, Stefflova K, Niedre MJ, Wilson BC, Chance B, Glickson JD, et al. Protease-triggered photosensitizing beacon based on singlet oxygen quenching and activation. *J Am Chem Soc.* 2004; 126: 11450-1.
 65. Fu LH, Wan Y, Li C, Qi C, He T, Yang C, et al. Biodegradable calcium phosphate nanotheranostics with tumor-specific activatable cascade catalytic reactions-augmented photodynamic therapy. *Adv. Funct. Mater.* 2021; 31: 2009848.
 66. Jiang M, Mu J, Jacobson O, Wang Z, He L, Zhang F, et al. Reactive oxygen species activatable heterodimeric prodrug as tumor-selective nanotheranostics. *ACS Nano.* 2020; 14, 16875-86.
 67. Li T, Yan L. Functional polymer nanocarriers for photodynamic therapy. *Pharmaceuticals (basel).* 2018; 11:133.
 68. Li L, Huh KM. Polymeric nanocarrier systems for photodynamic therapy. *Biomater Res.* 2014; 18:19.
 69. Bayer CL, Luke GP, Emelianov SY. Photoacoustic imaging for medical diagnostics. *Acoust Today.* 2012; 8:15-23.
 70. Ho CJH, Balasundaram G, Driessen W, McLaren R, Wong CL, Dinis US, et al. Multifunctional photosensitizer-based contrast agents for photoacoustic imaging. *Sci Rep.* 2014; 4: 5342.
 71. Mallidi S, Luke GP, Emelianov S. Photoacoustic imaging in cancer detection, diagnosis, and treatment guidance. *Trends Biotechnol.* 2011; 29: 213-21.
 72. Valluru KS, Willmann JK. Clinical photoacoustic imaging of cancer. *Ultrasonography.* 2016; 35: 267-80.
 73. Weber J, Beard PC, Bohndiek SE. Contrast agents for molecular photoacoustic imaging. *Nat Methods.* 2016; 13: 639-50.
 74. Li C, Mei E, Chen C, Li Y, Nugasur B, Hou L, et al. Gold-nanobipyramid-based nanotheranostics for dual-modality imaging-guided phototherapy. *ACS Appl Mater Interfaces.* 2020; 12 :12541-48.
 75. Chen Z, Deán-Ben XL, Gottschalk S, Razansky D. Performance of optoacoustic and fluorescence imaging in detecting deep-seated fluorescent agents. *Biomed Opt Express.* 2018; 9: 2229-39.
 76. Abuteen A, Zanganeh S, Akhigbe J, Samankumara LP, Aguirre A, Biswal N, et al. The evaluation of NIR-absorbing porphyrin derivatives as contrast agents in photoacoustic imaging. *Phys Chem Chem Phys.* 2013; 15: 18502-9.
 77. Attia ABE, Balasundaram G, Driessen W, Ntziachristos V, Olivo M. Phthalocyanine photosensitizers as contrast agents for in vivo photoacoustic tumor imaging. *Biomed Opt Express.* 2015; 6: 591-8.
 78. Macdonald TD, Liu TW, Zheng G. An MRI-sensitive, non-photobleachable porphyrin photoacoustic agent. *Angew Chem Int Ed Engl.* 2014; 53: 6956-9.
 79. Huynh E, Lovell JF, Helfield BL, Jeon M, Kim C, Goertz DE, et al. Porphyrin shell microbubbles with intrinsic ultrasound and photoacoustic properties. *J Am Chem Soc.* 2012; 134: 16464-7.
 80. Huynh E, Jin CS, Wilson BC, Zheng G. Aggregate enhanced trimodal porphyrin shell microbubbles for ultrasound, photoacoustic, and fluorescence imaging. *Bioconjug Chem.* 2014; 25: 796-801.
 81. Ng KK, Takada M, Harmatys K, Chen J, Zheng G. Chlorosome-inspired synthesis of templated metallochlorin-lipid nanoassemblies for biomedical applications. *ACS Nano.* 2016; 10: 4092-101.
 82. Gong H, Dong Z, Liu Y, Yin S, Cheng L, Xi W, et al. Engineering of multifunctional nano-micelles for combined photothermal and photodynamic therapy under the guidance of multimodal imaging. *Adv Funct Mater.* 2014; 24:6492-502.
 83. Feng L, Cheng L, Dong Z, Tao D, Barnhart TE, Cai W, et al. Theranostic liposomes with hypoxia-activated prodrug to effectively destruct hypoxic tumors post-photodynamic therapy. *ACS Nano.* 2017; 11: 927-37.
 84. Lin J, Wang S, Huang P, Wang Z, Chen S, Niu G, et al. Photosensitizer-loaded gold vesicles with strong plasmonic coupling effect for imaging-guided photothermal/photodynamic therapy. *ACS Nano.* 2013; 7: 5320-9.
 85. Ding H, Cai Y, Chen J, Lu T, Wen W, Nie G, et al. Cryodesiccation-driven crystallization preparation approach for zinc(II)-phthalocyanine nanodots in cancer photodynamic therapy and photoacoustic imaging. *Mikrochim Acta.* 2019; 186: 237.
 86. Siwawannapong K, Zhang R, Lei H, Jin Q, Tang W, Dong Z, et al. Ultra-small pyropheophorbide - a nanodots for near - infrared fluorescence/photoacoustic imaging-guided photodynamic therapy. *Theranostics.* 2020; 10: 62-73.
 87. Yan X, Hu H, Lin J, Jin AJ, Niu G, Zhang S, et al. Optical and photoacoustic dual-modality imaging guided synergistic photodynamic/photothermal therapies. *Nanoscale.* 2015; 7: 2520-6.
 88. Choi W, Oh D, Kim C. Practical photoacoustic tomography: Realistic limitations and technical solutions. *Appl. Phys. Rev.* 2020; 127: 230903.
 89. Yao J, Huang C, Liu C, Yang M. Upconversion luminescence nanomaterials: A versatile platform for imaging, sensing, and therapy. *Talanta.* 2020; 208: 120157.
 90. Qiu H, Tan M, Ohulchanskyy TY, Lovell JF, Chen G. Recent progress in upconversion photodynamic therapy. *Nanomaterials (Basel).* 2018; 8: 344.
 91. Liu Y, Meng X, Bu W. Upconversion-based photodynamic cancer therapy. *Coord Chem Rev.* 2019; 379: 82-98.
 92. Liang G, Wang H, Shi H, Wang H, Zhu M, Jing A, et al. Recent progress in the development of upconversion nanomaterials in bioimaging and disease treatment. *J Nanobiotechnology.* 2020; 18:154.
 93. Park YI, Kim HM, Kim JH, Moon KC, Yoo B, Lee KT, et al. Theranostic probe based on lanthanide-doped nanoparticles for simultaneous in vivo dual-modal imaging and photodynamic therapy. *Adv Mater.* 2012; 24: 5755-61.
 94. Huang WT, Chan MH, Chen X, Hsiao M, Liu RS. Theranostic nanobubble encapsulating a plasmon-enhanced upconversion hybrid nanosystem for cancer therapy. *Theranostics.* 2020; 10: 782-96.
 95. Wang S, Wei Z, Li L, Ning X, Liu Y. Luminescence imaging-guided triple-collaboratively enhanced photodynamic therapy by biospecific lanthanide-based nanomedicine. *Nanomedicine.* 2020; 29: 102265.
 96. Wang X, Yang CX, Chen JT, Yan XP. A dual-targeting upconversion nanoplatfor for two-color fluorescence imaging-guided photodynamic therapy. *Anal Chem.* 2014; 86: 3263-7.
 97. Lin B, Liu J, Wang Y, Yang F, Huang L, Lv R. Enhanced upconversion luminescence-guided synergistic antitumor therapy based on photodynamic therapy and immune checkpoint blockade. *Chem Mater.* 2020; 32: 4627-40.
 98. Guan M, Dong H, Ge J, Chen D, Sun L, Li S, et al. Multifunctional upconversion-nanoparticles-trimethylpyridylporphyrin-fullerene nanocomposite: a near-infrared light-triggered theranostic platform for imaging-guided photodynamic therapy. *NPG Asia Mater.* 2015; 7. e205.
 99. Feng M, Lv R, Xiao L, Hu B, Zhu S, He F, et al. Highly erbium-doped nanoplatfor with enhanced red emission for dual-modal optical-imaging-guided photodynamic therapy. *Inorg Chem.* 2018; 57: 14594-602.
 100. Zeng L, Xiang L, Ren W, Zheng J, Li T, Chen B, et al. Multifunctional photosensitizer-conjugated core-shell Fe₃O₄@NaYF₄:Yb/Er nano-complexes and their applications in T2-weighted magnetic resonance/upconversion luminescence imaging and photodynamic therapy of cancer cells. *RSC Adv.* 2013; 3: 13915-25.
 101. Feng Y, Wu Y, Zuo J, Tu L, Que I, Chang Y, et al. Assembly of upconversion nanophotosensitizer in vivo to achieve scatheless real-time imaging and selective photodynamic therapy. *Biomaterials.* 2019; 201: 33-41.
 102. Chen G, Shen J, Ohulchanskyy TY, Patel NJ, Kutikov A, Li Z, et al. (α-NaYbF₄:Tm(3+))/CaF₂ core/shell nanoparticles with efficient near-infrared to near-infrared upconversion for high-contrast deep tissue bioimaging. *ACS Nano.* 2012; 6: 8280-7.
 103. Del Rosal B, Jaque D. Upconversion nanoparticles for in vivo applications: limitations and future perspectives. *Methods Appl Fluoresc.* 2019; 7: 022001.

104. Andreou C, Kishore SA, Kircher MF. Surface-Enhanced Raman Spectroscopy: a new modality for cancer imaging. *J Nucl Med*. 2015; 56: 1295-9.
105. Sun C, Gao M, Zhang X. Surface-Enhanced Raman scattering (SERS) imaging-guided real-time photothermal ablation of target cancer cells using polydopamine-encapsulated gold nanorods as multifunctional agents. *Anal Bioanal Chem*. 2017; 409: 4915-26.
106. Murphy S, Huang L, Kamat PV. Charge-transfer complexation and excited-state interactions in porphyrin-silver nanoparticle hybrid structures. *J Phys Chem C*. 2011; 115: 22761-69.
107. Zhang Y, Aslan K, Previte MJR, Geddes CD. Metal-enhanced singlet oxygen generation: a consequence of plasmon enhanced triplet yields. *J Fluoresc*. 2007; 17: 345-9.
108. Khaing Oo MK, Yang Y, Hu Y, Gomez M, Du H, Wang H. Gold nanoparticle-enhanced and size-dependent generation of reactive oxygen species from protoporphyrin IX. *ACS Nano*. 2012; 6: 1939-47.
109. Zhang Z, Wang S, Xu H, Wang B, Yao C. Role of 5-aminolevulinic acid-conjugated gold nanoparticles for photodynamic therapy of cancer. *J Biomed Opt*. 2015; 20: 51043.
110. Gao Y, Li Y, Chen J, Zhu S, Liu X, Zhou L, et al. Multifunctional gold nanostar-based nanocomposite: Synthesis and application for noninvasive MR-SERS imaging-guided photothermal ablation. *Biomaterials*. 2015; 60: 31-41.
111. Liu Y, Chang Z, Yuan H, Fales AM, Vo-Dinh T. Quintuple-modality (SERS-MRI-CT-TPL-PTT) plasmonic nanoprobe for theranostics. *Nanoscale*. 2013; 5: 12126-31.
112. von Maltzahn G, Centrone A, Park JH, Ramanathan R, Sailor MJ, Hatton TA, et al. SERS-coded gold nanorods as a multifunctional platform for densely multiplexed near-infrared imaging and photothermal heating. *Adv Mater*. 2009; 21: 3175-180.
113. Liu Y, Ashton JR, Moding EJ, Yuan H, Register JK, Fales AM, et al. A plasmonic gold nanostar theranostic probe for in vivo tumor imaging and photothermal therapy. *Theranostics*. 2015; 5: 946-60.
114. Tang P, Xing M, Xing X, Tao Q, Cheng W, Liu S, et al. Receptor-mediated photothermal/photodynamic synergistic anticancer nanodrugs with SERS tracing function. *Colloids Surf B Biointerfaces*. 2021; 199: 111550.
115. Zhang Y, Qian J, Wang D, Wang Y, He S. Multifunctional gold nanorods with ultrahigh stability and tunability for in vivo fluorescence imaging, SERS detection, and photodynamic therapy. *Angew Chem Int Ed Engl*. 2013; 52: 1148-51.
116. Fales AM, Yuan H, Vo-Dinh T. Silica-coated gold nanostars for combined surface-enhanced Raman scattering (SERS) detection and singlet-oxygen generation: a potential nanoplatform for theranostics. *Langmuir*. 2011; 27: 12186-90.
117. Tam NCM, McVeigh PZ, MacDonald TD, Farhadi A, Wilson BC, Zheng G. Porphyrin-lipid stabilized gold nanoparticles for surface enhanced Raman scattering based imaging. *Bioconjug Chem*. 2012; 23: 1726-30.
118. Farhadi A, Roxin A, Wilson BC, Zheng G. Nano-enabled SERS reporting photosensitizers. *Theranostics*. 2015; 5: 469-76.
119. Li Y, Wei Q, Ma F, Li X, Liu F, Zhou M. Surface-enhanced Raman nanoparticles for tumor theranostics applications. *Acta Pharm Sin B*. 2018; 8: 349-59.
120. Sour A, Jenni S, Ortí-Suárez A, Schmitt J, Heitz V, Bolze F, et al. Four gadolinium(III) complexes appended to a porphyrin: a water-soluble molecular theranostic agent with remarkable relaxivity suited for mri tracking of the photosensitizer. *Inorg Chem*. 2016; 55: 4545-54.
121. Xiao YD, Paudel R, Liu J, Ma C, Zhang ZS, Zhou SK. MRI contrast agents: classification and application (Review). *Int J Mol Med*. 2016; 38: 1319-26.
122. Vaidya A, Sun Y, Ke T, Jeong EK, Lu ZR. Contrast enhanced MRI-guided photodynamic therapy for site-specific cancer treatment. *Magn Reson Med*. 2006; 56: 761-7.
123. Chen CW, Cohen JS, Myers CE, Sohn M. Paramagnetic metalloporphyrins as potential contrast agents in NMR imaging. *FEBS Lett*. 1984; 168: 70-4.
124. Furmanski P, Longley C. Metalloporphyrin enhancement of magnetic resonance imaging of human tumor xenografts in nude mice. *Cancer Res*. 1988; 48: 4604-10.
125. Fiel RJ, Musser DA, Mark EH, Mazurchuk R, Alletto JJ. A comparative study of manganese meso-sulfonatophenyl porphyrins: contrast-enhancing agents for tumors. *Magn Reson Imaging*. 1990; 8: 255-9.
126. Takehara Y, Sakahara H, Masunaga H, Isogai S, Kodaira N, Takeda H, et al. Tumour enhancement with newly developed Mn-metalloporphyrin (HOP-9P) in magnetic resonance imaging of mice. *Br J Cancer*. 2001; 84: 1681-5.
127. Pan D, Caruthers SD, Senpan A, Schmieder AH, Wickline SA, Lanza GM. Revisiting an old friend: manganese-based MRI contrast agents. *Wiley Interdiscip Rev Nanomed Nanobiotechnol*. 2011; 3: 162-73.
128. Zou T, Zhen M, Chen D, Li R, Guan M, Shu C, et al. The positive influence of fullerene derivatives bonded to manganese(III) porphyrins on water proton relaxation. *Dalton Trans*. 2015; 44: 9114-9.
129. Aime S, Botta M, Gianolio E, Terreno E. A p(O₂)-responsive mri contrast agent based on the redox switch of manganese (II / III) - porphyrin complexes. *Angew Chem Int Ed Engl*. 2000; 39: 747-50.
130. Ni Y. Metalloporphyrins and functional analogues as MRI contrast agents. *Curr Med Imaging*. 2008; 4: 96-112.
131. Sessler JL, Mody TD, Hemmi GW, Lynch V, Young SW, Miller RA. Gadolinium(III) texaphyrin: a novel MRI contrast agent. *J Am Chem Soc*. 1993; 115: 10368-9.
132. Young SW, Qing F, Harriman A, Sessler JL, Dow WC, Mody TD, et al. Gadolinium(III) texaphyrin: a tumor selective radiation sensitizer that is detectable by MRI. *Proc Natl Acad Sci U S A*. 1996; 93: 6610-5.
133. Yuzhakova DV, Lermontova SA, Grigoryev IS, Muravieva MS, Gavrina AI, Shirmanova MV, et al. In vivo multimodal tumor imaging and photodynamic therapy with novel theranostic agents based on the porphyrine framework-chelated gadolinium (III) cation. *Biochim Biophys Acta Gen Subj*. 2017; 1861: 3120-30.
134. Jenni S, Bolze F, Bonnet CS, Pallier A, Sour A, Tóth É, et al. Synthesis and in vitro studies of a Gd(DOTA)-porphyrin conjugate for combined MRI and photodynamic treatment. *Inorg Chem*. 2020; 59: 14389-98.
135. Hofmann B, Bogdanov A, Marecos E, Ebert W, Semmler W, Weissleder R. Mechanism of gadophrin-2 accumulation in tumor necrosis. *J Magn Reson Imaging*. 1999; 9: 336-41.
136. Barkhausen J, Ebert W, Debatin JF, Weinmann HJ. Imaging of myocardial infarction: comparison of magnevist and gadophrin-3 in rabbits. *J Am Coll Cardiol*. 2002; 39: 1392-8.
137. Metz S, Daldrop-Link HE, Richter T, Räch C, Ebert W, Settles M, et al. Detection and quantification of breast tumor necrosis with MR imaging: value of the necrosis-avid contrast agent Gadophrin-3. *Acad Radiol*. 2003; 10: 484-90.
138. Daldrop-Link HE, Rudelius M, Metz S, Piontek G, Fichier B, Settles M, et al. Cell tracking with gadophrin-2: a bifunctional contrast agent for MR imaging, optical imaging, and fluorescence microscopy. *Eur J Nucl Med Mol Imaging*. 2004; 31:1312-21.
139. Ni Y, Petré C, Miao Y, Yu J, Cresens E, Adriaens P, et al. Magnetic resonance imaging-histomorphologic correlation studies on paramagnetic metalloporphyrins in rat models of necrosis. *Invest Radiol*. 1997; 32: 770-9.
140. Haroon-Ur-Rashid, Umar K Khan MN, Anjum MN, Yaseen M. Synthesis and relaxivity measurement of porphyrin-based Magnetic Resonance Imaging (MRI) contrast agents. *J Struct Chem*. 2014; 55:910-5.
141. Gros CP, Eggenspiller A, Nonat A, Barbe JM, Denat F. New potential bimodal imaging contrast agents based on DOTA-like and porphyrin macrocycles. *Medchemcomm*. 2011; 2: 119-25.
142. Eggenspiller A, Michelin C, Desbois N, Richard P, Barbe JM, Denat F, et al. Design of Porphyrin-dota-Like Scaffolds as All-in-One Multimodal Heterometallic Complexes for Medical Imaging. *European J Org Chem*. 2013:6629-43.
143. Trivedi ER, Ma Z, Waters EA, Macrenaris KW, Subramanian R, Barrett AGM, et al. Synthesis and characterization of a porphyrine-Gd(III) MRI contrast agent and in vivo imaging of a breast cancer xenograft model. *Contrast Media Mol Imaging*. 2014; 9: 313-22.
144. Hindré F, Le Plouzennec M, de Certaines JD, Foultier MT, Patrice T, Simonneaux G. Tetra-p-aminophenylporphyrin conjugated with Gd-DTPA: tumor-specific contrast agent for MR imaging. *J Magn Reson Imaging*. 1993; 3: 59-65.
145. Li G, Slansky A, Dobhal MP, Goswami LN, Graham A, Chen Y, et al. Chlorophyll-a analogues conjugated with aminobenzyl-DTPA as potential bifunctional agents for magnetic resonance imaging and photodynamic therapy. *Bioconjug Chem*. 2005: 32-42.
146. Pandey SK, Sajjad M, Chen Y, Zheng X, Yao R, Missert JR, et al. Comparative positron-emission tomography (PET) imaging and phototherapeutic potential of 124I- labeled methyl- 3-(1'-iodobenzoyloxyethyl)pyropheophorbide-a vs the corresponding glucose and galactose conjugates. *J Med Chem*. 2009; 52: 445-55.
147. Song Y, Zong H, Trivedi ER, Vesper BJ, Waters EA, Barrett AGM, et al. Synthesis and characterization of new porphyrine-Gd(III) conjugates as multimodal MR contrast agents. *Bioconjug Chem*. 2010; 21: 2267-75.
148. Tekdaş DA, Garifullin R, Şentürk B, Zorlu Y, Gundogdu U, Atalar E, et al. Design of a Gd-DOTA-phthalocyanine conjugate combining MRI contrast imaging and photosensitization properties as a potential molecular theranostic. *Photochem Photobiol*. 2014; 90: 1376-86.
149. Wu B, Li XQ, Huang T, Lu ST, Wan B, Liao RF, et al. MRI-guided tumor chemo-photodynamic therapy with Gd/Pt bifunctionalized porphyrin. *Biomater Sci*. 2017; 5: 1746-50.
150. Schmitt J, Heitz V, Sour A, Bolze F, Kessler P, Flamigni L, et al. A theranostic agent combining a two-photon-absorbing photosensitizer for photodynamic therapy and a Gadolinium(III) complex for MRI detection. *Chemistry*. 2016; 22: 2775-86.
151. Schmitt J, Jenni S, Sour A, Heitz V, Bolze F, Pallier A, et al. A porphyrin dimer-GdDOTA conjugate as a theranostic agent for one- and two-photon photodynamic therapy and MRI. *Bioconjug Chem*. 2018; 29: 3726-38.
152. Sivasubramanian M, Chuang YC, Lo LW. Evolution of nanoparticle-mediated photodynamic therapy: from superficial to deep-seated cancers. *Molecules*. 2019; 24:520.
153. Jahanbin T, Sauriat-Dorizon H, Spearman P, Benderbous S, Korri-Youssoufi H. Development of Gd(III) porphyrin-conjugated chitosan nanoparticles as contrast agents for magnetic resonance imaging. *Mater Sci Eng C Mater Biol Appl*. 2015; 52: 325-32.
154. Jing L, Liang X, Li X, Lin L, Yang Y, Yue X, et al. Mn-porphyrin conjugated Au nanoshells encapsulating doxorubicin for potential magnetic resonance

- imaging and light triggered synergistic therapy of cancer. *Theranostics*. 2014; 4: 858-71.
155. Huang P, Li Z, Lin J, Yang D, Gao G, Xu C, et al. Photosensitizer-conjugated magnetic nanoparticles for *in vivo* simultaneous magnetofluorescent imaging and targeting therapy. *Biomaterials*. 2011; 32: 3447-58.
156. Ostroverkhov P, Semkina A, Naumenko V, Plotnikova E, Yakubovskaya R, Vodopyanov S, et al. HSA-coated magnetic nanoparticles for MRI-guided photodynamic cancer therapy. *Pharmaceutics*. 2018; 10: 284.
157. Nowostawska M, Corr SA, Byrne SJ, Conroy J, Volkov Y, Gun'ko YK. Porphyrin-magnetite nanoconjugates for biological imaging. *J Nanobiotechnology* 2011; 9:13.
158. Millán JG, Brasch M, Anaya-Plaza E, de la Escosura A, Velders AH, Reinhoudt DN, et al. Self-assembly triggered by self-assembly: optically active, paramagnetic micelles encapsulated in protein cage nanoparticles. *J Inorg Biochem*. 2014; 136: 140-6.
159. Qazi S, Uchida M, Usselman R, Shearer R, Edwards E, Douglas T. Manganese(III) porphyrins complexed with P22 virus-like particles as T1-enhanced contrast agents for magnetic resonance imaging. *J Biol Inorg Chem*. 2014; 19: 237-46.
160. Zhou L, Yang T, Wang J, Wang Q, Lv X, Ke H, et al. Size-tunable Gd₂O₃@albumin nanoparticles conjugating Chlorin e6 for magnetic resonance imaging-guided photo-induced therapy. *Theranostics*. 2017; 7: 764-74.
161. Arms L, Smith DW, Flynn J, Palmer W, Martin A, Woldu A, et al. Advantages and limitations of current techniques for analyzing the biodistribution of nanoparticles. *Front Pharmacol*. 2018; 9: 802.
162. Almuhaideb A, Papathanasiou N, Bomanji J. 18F-FDG PET/CT imaging in oncology. *Ann Saudi Med*. 2011; 31: 3-13.
163. Cauchon N, Turcotte E, Lecomte R, Hasséssian HM, Lier JEV. Predicting efficacy of photodynamic therapy by real-time FDG-PET in a mouse tumour model. *Photochem Photobiol Sci*. 2012; 11: 364-70.
164. Kharroubi Lakouas D, Huglo D, Mordon S, Vermandel M. Nuclear medicine for photodynamic therapy in cancer: Planning, monitoring and nuclear PDT. *Photodiagnosis Photodyn Ther*. 2017; 18: 236-43.
165. Waghorn PA. Radiolabelled porphyrins in nuclear medicine. *J Labelled Comp Radiopharm*. 2014; 57: 304-9.
166. Firnau G, Maass D, Wilson BC, Jeeves WP. ⁶⁴Cu labelling of hematoporphyrin derivative for non-invasive *in vivo* measurements of tumour uptake. *Prog Clin Biol Res*. 1984; 170: 629-36.
167. Wilson BC, Firnau G, Jeeves WP, Brown KL, Burns-McCormick DM. Chromatographic analysis and tissue distribution of radiocopper-labelled haematoporphyrin derivatives. *Laser Med Sci*. 1988; 3:71-80.
168. Shi J, Liu TWB, Chen J, Green D, Jaffray D, Wilson BC, et al. Transforming a targeted porphyrin theranostic agent into a pet imaging probe for cancer. *Theranostics*. 2011; 1: 363-70.
169. Aguilar-Ortiz E, Jalilian AR, Ávila-Rodríguez MA. Porphyrins as ligands for ⁶⁴copper: background and trends. *Medchemcomm*. 2018; 9: 1577-88.
170. Soucy-Faulkner A, Rousseau JA, Langlois R, Bernard V, Lecomte R, Bénéard F, et al. Copper-64 labeled sulfophthalocyanines for positron emission tomography (PET) imaging in tumor-bearing rats. *J Porphyr Phthalocyanines*. 2008; 12: 49-53.
171. Fazaeli Y, Jalilian AR, Amini MM, Aboudzadeh M, Feizi S, Rahiminezhad A, et al. Preparation, nano purification, quality control and labeling optimization of [⁶⁴Cu]-5,10,15,20-tetrakis (penta fluoro phenyl) porphyrin complex as a possible imaging agent. *J Radioanal Nucl Chem*. 2013; 295: 255-63.
172. Ranyuk ER, Cauchon N, Ali H, Lecomte R, Guérin B, Van Lier JE. PET imaging using ⁶⁴Cu-labeled sulfophthalocyanines: synthesis and biodistribution. *Bioorg Med Chem Lett*. 2011; 21: 7470-3.
173. Rong P, Yang K, Srivastan A, Kiesewetter DO, Yue X, Wang F, et al. Photosensitizer loaded nano-graphene for multimodality imaging guided tumor photodynamic therapy. *Theranostics*. 2014; 4: 229-39.
174. Liu TW, MacDonald TD, Shi J, Wilson BC, Zheng G. Intrinsically copper-64-labeled organic nanoparticles as radiotracers. *Angew Chem Int Ed Engl*. 2012; 51: 13128-31.
175. Moran M, MacDonald T, Liu T, Forbes J, Zheng G, Valliant J. Copper-64-labeled porphyrins for PET imaging. *J Nucl Med*. 2014; 55: 1016 (supplement 1).
176. Huang H, Hernandez R, Geng J, Sun H, Song W, Chen F, et al. A porphyrin-PEG polymer with rapid renal clearance. *Biomaterials*. 2016; 76: 25-32.
177. Zhang Y, Wang D, Goel S, Sun B, Chitgupi U, Geng J, et al. Surfactant-stripped frozen pheophytin micelles for multimodal gut imaging. *Adv Mater*. 2016; 28: 8524-30.
178. Li Y, Lin TY, Luo Y, Liu Q, Xiao W, Guo W, et al. A smart and versatile theranostic nanomedicine platform based on nanoporphyrin. *Nat Commun*. 2014; 5: 4712.
179. Li Z, Lin TP, Liu S, Huang CW, Hudnall TW, Gabbai FP, et al. Rapid aqueous [¹⁸F]-labeling of a bodipy dye for positron emission tomography/fluorescence dual modality imaging. *Chem Commun (Camb)*. 2011; 47: 9324-6.
180. Chen Y, Sajjad M, Wang Y, Batt C, Nabi HA, Pandey RK. TSP0 18 kDa (PBR) targeted photosensitizers for cancer imaging (PET) and PDT. *ACS Med Chem Lett*. 2011; 2: 136-41.
181. Pandey SK, Sajjad M, Chen Y, Pandey A, Missert JR, Batt C, et al. Compared to purpurinimides, the pyropheophorbide containing an iodobenzyl group showed enhanced PDT efficacy and tumor imaging (¹²⁴I-PET) ability. *Bioconjug Chem*. 2009; 20: 274-82.
182. Tamura M, Matsui H, Hirohara S, Kakiuchi K, Tanihara M, Takahashi N, et al. Selective accumulation of [⁶⁷Zn]-labeled glycoconjugated porphyrins as multi-functional positron emission tomography tracers in cancer cells. *Bioorg Med Chem*. 2014; 22: 2563-70.
183. Peng CL, Shih YH, Lee PC, Hsieh TMH, Luo TY, Shieh MJ. Multimodal image-guided photothermal therapy mediated by 188Re-labeled micelles containing a cyanine-type photosensitizer. *ACS Nano*. 2011; 5: 5594-607.
184. Fazaeli Y, Jalilian AR, Amini MM, Rahiminejad-Kisomi A, Rajabifar S, Bolourinovin F, et al. Preparation and preliminary evaluation of [⁶⁷Ga]-tetra phenyl porphyrin complexes as possible imaging agents. *J Radioanal Nucl Chem*. 2011; 288: 17-24.
185. Sadeghi S, Mirzaei M, Rahimi M, Jalilian AR. Development of (111)In-labeled porphyrins for SPECT imaging. *Asia Ocean J Nucl Med Biol*. 2014; 2: 95-103.
186. Lee JH, Shao S, Cheng KT, Lovell JF, Paik CH. (99m)Tc-labeled porphyrin-lipid nanovesicles. *J Liposome Res*. 2015; 25: 101-6.
187. Origiano TC, Karesh SM, Jenkin RE, Halama JR, Reichman OH. Photodynamic therapy for intracranial neoplasms: investigations of photosensitizer uptake and distribution using indium-111 Photofrin-II single photon emission computed tomography scans in humans with intracranial neoplasms. *Neurosurgery*. 1993; 32: 357-63.
188. Blum NT, Zhang Y, Qu J, Lin J, Huang P. Recent advances in self-exciting photodynamic therapy. *Front Bioeng Biotechnol*. 2020;8: 594491.
189. Kiessling F, Fokong S, Bzyl J, Lederle W, Palmowski M, Lammers T. Recent advances in molecular, multimodal and theranostic ultrasound imaging. *Adv Drug Deliv Rev*. 2014; 72: 15-27.
190. Cornelis FH, Kim K, Durack JC, Jebiwott S, Scherz A, Srimathveeravalli G, et al. Contrast enhanced ultrasound imaging can predict vascular-targeted photodynamic therapy induced tumor necrosis in small animals. *Photodiagnosis Photodyn Ther*. 2017; 20: 165-8.
191. Park DJ, Min KH, Lee HJ, Kim K, Kwon IC, Jeong SY, et al. Photosensitizer-loaded bubble-generating mineralized nanoparticles for ultrasound imaging and photodynamic therapy. *J Mater Chem B*. 2016; 4: 1219-27.
192. Huynh E, Leung BYC, Helfield BL, Shakiba M, Gandier JA, Jin CS, et al. *In situ* conversion of porphyrin microbubbles to nanoparticles for multimodality imaging. *Nat Nanotechnol*. 2015; 10: 325-32.
193. You Y, Liang X, Yin T, Chen M, Qiu C, Gao C, et al. Porphyrin-grafted lipid microbubbles for the enhanced efficacy of photodynamic therapy in prostate cancer through ultrasound-controlled *in situ* accumulation. *Theranostics*. 2018; 8: 1665-77.
194. Svenskaya YI, Navolokin NA, Bucharskaya AB, Terentyuk GS, Kuz'mina AO, Burashnikova MM, et al. Calcium carbonate microparticles containing a photosensitizer photosens: Preparation, ultrasound stimulated dye release, and *in vivo* application. *Nanotechnol Russia*. 2014; 9: 398-409.
195. Fan W, Qi Y, Wang R, Xu C, Zhao N, Xu FJ. Calcium carbonate-methylene blue nanohybrids for photodynamic therapy and ultrasound imaging. *Sci China Life Sci*. 2018; 61: 483-91.
196. Huang Y, Shen K, Si Y, Shan C, Guo H, Chen M, et al. Dendritic organosilica nanospheres with large mesopores as multi-guests vehicle for photoacoustic/ultrasound imaging-guided photodynamic therapy. *J Colloid Interface Sci*. 2021; 583: 166-77.
197. Sun S, Xu Y, Fu P, Chen M, Sun S, Zhao R, et al. Ultrasound-targeted photodynamic and gene dual therapy for effectively inhibiting triple negative breast cancer by cationic porphyrin lipid microbubbles loaded with HIF1 α -siRNA. *Nanoscale*. 2018; 10: 19945-56.
198. Zheng Y, Yeb J, Li Z, Chen H, Gao Y. Recent progress in sono-photodynamic cancer therapy: From developed new sensitizers to nanotechnology-based efficacy enhancing strategies. *Acta Pharm Sin B*. 2020; In Press.
199. Forrest LJ. Computed tomography imaging in oncology. *Vet Clin North Am Small Anim Pract*. 2016; 46: 499-513.
200. Yin HQ, Cao PP, Wang XY, Li YH, Yin XB. Computed tomography imaging-guided tandem catalysis-enhanced photodynamic therapy with gold nanoparticle functional covalent organic polymers. *ACS Appl Bio Mater*. 2020; 3: 2534-42.
201. Xu H, Ohulchanskyy TY, Yakovliev A, Zinyuk R, Song J, Liu L, et al. Nanoliposomes co-encapsulating ct imaging contrast agent and photosensitizer for enhanced, imaging guided photodynamic therapy of cancer. *Theranostics*. 2019; 9: 1323-35.
202. Zhang L, Li M, Zhou Q, Dang M, Tang Y, Wang S, et al. Computed tomography and photoacoustic imaging guided photodynamic therapy against breast cancer based on mesoporous platinum with insitu oxygen generation ability. *Acta Pharm Sin B*. 2020; 10: 1719-29.
203. Liu L, Wang J, You Q, Sun Q, Song Y, Wang Y, et al. NIRF/PA/CT multi-modality imaging guided combined photothermal and photodynamic therapy based on tumor microenvironment-responsive nanocomposites. *J Mater Chem B*. 2018; 6: 4239-50.
204. Yang L, Wang J, Yang S, Lu Q, Li P, Li N. Rod-shape MSN@MoS₂ Nanoplatform for FL/MSOT/CT imaging-guided photothermal and photodynamic therapy. *Theranostics*. 2019; 9: 3992-4005.
205. Li B, Zhou Q, Wang H, Zha Y, Zheng P, Yang T, et al. Mitochondria-targeted magnetic gold nanoheterostructure for multi-modal imaging guided

- photothermal and photodynamic therapy of triple-negative breast cancer. *Chem Eng J.* 2020; 403: 126364.
206. Liu L, Wang J, Tan X, Pang X, You Q, Sun Q, et al. Photosensitizer loaded PEG-MoS₂-Au hybrids for CT/NIRF imaging-guided stepwise photothermal and photodynamic therapy. *J Mater Chem B.* 2017; 5: 2286-96.
207. Yang S, You Q, Yang L, Li P, Lu Q, Wang S, et al. Rodlike MSN@Au nanohybrid-modified supermolecular photosensitizer for NIRF/MSOT/CT/MR quadmodal imaging-guided photothermal/photodynamic cancer therapy. *ACS Appl Mater Interfaces.* 2019; 11: 6777-88.
208. Xu H, Ohulchanskyy TY, Qu J. Nanoliposomes for photodynamic therapy guided by fluorescence and computed tomography imaging. *International Conference on Photonics and Imaging in Biology and Medicine. Optical Society of America, 2017.W3A.25.*
209. Rao NV, Ko H, Lee J, Park JH. Recent progress and advances in stimuli-responsive polymers for cancer therapy. *Front Bioeng Biotechnol.* 2018; 6:110.
210. Chiba M, Ichikawa Y, Kamiya M, Komatsu T, Ueno T, Hanaoka K, et al. An activatable photosensitizer targeted to γ -glutamyltranspeptidase. *Angew Chem Int Ed Engl.* 2017; 56:10418-22.
211. Chiba M, Kamiya M, Tsuda-Sakurai K, Fujisawa Y, Kosakamoto H, Kojima R, et al. Activatable photosensitizer for targeted ablation of *lacZ*-positive cells with single-cell resolution. *ACS Cent Sci.* 2019; 5: 1676-81.
212. Wang Y, Wu W, Liu J, Manghnani PN, Hu F, Ma D, et al. Cancer-cell-activated photodynamic therapy assisted by Cu(II)-based metal-organic framework. *ACS Nano.* 2019; 13: 6879-90.
213. Tian J, Zhou J, Shen Z, Ding L, Yu JS, Ju H. A pH-activatable and aniline-substituted photosensitizer for near-infrared cancer theranostics. *Chem Sci.* 2015; 6: 5969-77.
214. Battogtokh G, Ko YT. Active-targeted pH-responsive albumin-photosensitizer conjugate nanoparticles as theranostic agents. *J Mater Chem B.* 2015; 3: 9349-59.
215. Li X, Zheng BY, Ke MR, Zhang Y, Huang JD, Yoon J. A tumor-pH-responsive supramolecular photosensitizer for activatable photodynamic therapy with minimal in vivo skin phototoxicity. *Theranostics.* 2017; 7: 2746-56.
216. Fang S, Lin J, Li C, Huang P, Hou W, Zhang C, et al. Dual-stimuli responsive nanotheranostics for multimodal imaging guided trimodal synergistic therapy. *Small.* 2017; 13: 1602580.
217. Gao S, Wang G, Qin Z, Wang X, Zhao G, Ma Q, et al. Oxygen-generating hybrid nanoparticles to enhance fluorescent/photoacoustic/ultrasound imaging guided tumor photodynamic therapy. *Biomaterials.* 2017; 112: 324-35.
218. Li W, Zheng C, Pan Z, Chen C, Hu D, Gao G, et al. Smart hyaluronidase-activated theranostic micelles for dual-modal imaging guided photodynamic therapy. *Biomaterials.* 2016; 101: 10-19.
219. Yang X, Shi X, Ji J, Zhai G. Development of redox-responsive theranostic nanoparticles for near-infrared fluorescence imaging-guided photodynamic/chemotherapy of tumor. *Drug Deliv.* 2018; 25: 780-96.
220. Liu P, Yue C, Sheng Z, Gao G, Li M, Yi H, et al. Photosensitizer-conjugated redox-responsive dextran theranostic nanoparticles for near-infrared cancer imaging and photodynamic therapy. *Polym Chem.* 2014; 5: 874-81.
221. Cho MH, Li Y, Lo PC, Lee H, Choi Y. Fucoidan-based theranostic nanogel for enhancing imaging and photodynamic therapy of cancer. *Nano-Micro Lett.* 2020; 12: 47.
222. Tong H, Chen Y, Li Z, Li H, Chen T, Jin Q, et al. Glutathione activatable photosensitizer-conjugated pseudopolyrotaxane nanocarriers for photodynamic theranostics. *Small.* 2016; 12: 6223-32.
223. Wang D, Zhang N, Jing X, Zhang Y, Xu Y, Meng L. A tumor-microenvironment fully responsive nano-platform for MRI-guided photodynamic and photothermal synergistic therapy. *J Mater Chem B.* 2020; 8: 8271-81.
224. Zeng Q, Zhang R, Zhang T, Xing D. H₂O₂-responsive biodegradable nanomedicine for cancer-selective dual-modal imaging guided precise photodynamic therapy. *Biomaterials.* 2019; 207: 39-48.
225. Du W, Liu T, Xue F, Chen Y, Chen Q, Luo Y, et al. Confined nanoparticles growth within hollow mesoporous nanoreactors for highly efficient MRI-guided photodynamic therapy. *Chem Eng J.* 2020; 379: 122251.
226. Ma Z, Jia X, Bai J, Ruan Y, Wang C, Li J, et al. MnO₂ gatekeeper: an intelligent and O₂-evolving shell for preventing premature release of high cargo payload core, overcoming tumor hypoxia, and acidic H₂O₂-sensitive MRI. *Adv Funct Mater.* 2017; 27: 1604258.
227. Hou W, Xia F, Alves CS, Qian X, Yang Y, Cui D. MMP2-targeting and redox-responsive pegylated chlorin e6 nanoparticles for cancer near-infrared imaging and photodynamic therapy. *ACS Appl Mater Interfaces.* 2016; 8: 1447-57.
228. Li X, Yu S, Lee Y, Guo T, Kwon N, Lee D, et al. In vivo albumin traps photosensitizer monomers from self-assembled phthalocyanine nanovesicles: a facile and switchable theranostic approach. *J Am Chem Soc.* 2019; 141:1366-72.
229. Li X, Yu S, Lee D, Kim G, Lee B, Cho Y, et al. Facile supramolecular approach to nucleic-acid-driven activatable nanotheranostics that overcome drawbacks of photodynamic therapy. *ACS Nano.* 2018; 12:681-88.
230. Li X, Kim CY, Lee S, Lee D, Chung HM, Kim G, et al. Nanostructured phthalocyanine assemblies with protein-driven switchable photoactivities for biophotonic imaging and therapy. *J Am Chem Soc.* 2017; 139:10880-6.
231. Sun Y, Zhang Y, Gao Y, Wang P, He G, Blum NT, et al. Six birds with one stone: versatile nanoporphyrin for single-laser-triggered synergistic phototheranostics and robust immune activation. *Adv Mater.* 2020; 32: e2004481.
232. Zhang Y, Bo S, Feng T, Qin X, Wan Y, Jiang S, et al. A versatile theranostic nanoemulsion for architecture-dependent multimodal imaging and dually augmented photodynamic therapy. *Adv Mater.* 2019; 31: e1806444.
233. Huang Y, He S, Cao W, Cai K, Liang XJ. Biomedical nanomaterials for imaging-guided cancer therapy. *Nanoscale.* 2012; 4: 6135-49.